

**APPENDIX A**  
**LITERATURE REVIEW TABLES**

Table A.1. Summary of pile group lateral load tests.

Reference	Lateral Load Test Description	Foundation Soil	Principal Findings
Feagin, L.B. (1937) and Feagin, L.B. (1948) and Feagin, L.B. (1953) and Gleser, S.M. (1953)	Conducted <b>full-scale field tests</b> on pile-supported locks and dams at locations along the Mississippi River. Tested groups of 14-in.-dia. timber piles driven vertically and battered at 3D to 4D spacing. Vertical piles were driven 30 ft and pile heads were constrained with concrete caps.	fine to coarse sand with occasional gravel	Observed that lateral movements of large pile groups is greater than that indicated by equivalent load tests on individual piles. Determined that groups combining both vertical and battered piles were more resistant than groups containing only vertical piles. The resistance increased as batter ratio increased. The greatest resistance was measured when vertical and lateral loads were combined, with the direction of lateral load the same as the direction of batter.
O'Halloran, J. (1953)	Conducted <b>full-scale field tests</b> (in 1928) on 2 pile groups in conjunction with the Anglo-Canadian Pulp and Paper Mill Project on the St. Charles River in Quebec City, Canada. The groups consisted of 4 fixed-head, 13 to 16-in.-dia., 21-ft-long timber piles.	sand fill, no strength data available	This constitutes one of the oldest group load tests on record. Group interaction effects were only qualitatively considered in the tests. The author and reviewers were surprised at the uncharacteristically high resistance of the 4-pile group, based on the load per pile in the group. They neglected passive resistance of the embedded 4-ft-deep pile cap.
Tschebotarioff, G.P. (1953)	Conducted <b>1g model tests</b> on 3-pile and 7-pile groups using 2-in.-dia., 29-in.-long wood piles, battered at 5 to 10 degrees.	14 in of well-graded fine sand underlain by 15 in of very soft silty clay	Determined that the magnitude and nature of stresses in a laterally loaded pile are related to the pile location within a group and the size of the group. Concluded that more experimental and analytical work is needed in this area.

Table A.1. Continued.

Reference	Lateral Load Test Description	Foundation Soil	Principal Findings
Wen, R.K. (1955)	Conducted <b>1g model tests</b> using three 45-in-long, 1.5 –in-square, white oak timber piles.	dry sand placed in a 2.5 by 6 by 4 ft deep wood tank	Observed that at high lateral loads, the front piles took the greatest portion of load and were the most severely stressed by bending.
Prakash, S. Saran, D. (1967)	Conducted <b>1g model tests</b> on 4-pile and 9-pile groups at spacings ranging from 3D to 5D. Model piles were 9-mm-dia., 11.4-in-long aluminum tubes. Pile heads were constrained by a 1-in-thick concrete pile cap. Test tank size was 10 by 6 by 12 in deep.	cohesive soil (ML) placed by dropping from a height of 4 ft, piles were pushed into tank	Determined that as pile spacing decreases in the direction of load, group rotation and deflection increases. Concluded that pile group effects vanish at spacings exceeding 6 pile diameters.
Alizadeh, M. Davisson, M.T. (1970)	Conducted 37 <b>full-scale field tests</b> in conjunction with the Arkansas River Navigation Project at Lock and Dam 1, 3, and 4 in the Arkansas River Valley. A variety of pile types including timber, prestressed concrete, steel pipe, and steel H-piles were tested free-headed.	alluvial soils consisting of fine sand and silty sand	Determined that a reasonable approximation can be obtained by assuming a triangular variation of the horizontal subgrade modulus ( $n_h$ ) with depth. Determined that $n_h$ is insensitive to deflections for deflections > 0.25 in, and strongly dependent on deflections when deflections are < 0.25 in. Small changes in $D_r$ can cause large changes in $n_h$ .

Table A.1. Continued.

Reference	Lateral Load Test Description	Foundation Soil	Principal Findings
Davisson, M.T. Salley, J.R. (1970)	Conducted <b>1g model tests</b> in conjunction with the Arkansas River Navigation Project on vertical and battered fixed-headed piles fabricated from 0.5-inch-O.D. aluminum tubing. Tested a 6-pile group constrained at the top by a cap, 2 scaled model lock walls supported on piles, and 3 scaled model dam monoliths supported on battered piles.	sand in a 4 by 4 by 4-ft.-deep tank, piles were embedded 21 in	Examined a variety of pile spacings. Determined that group effects decreased the effective value of the coefficient of subgrade reaction, $n_h$ , and increased the relative stiffness factor, $T$ . Measured normalized $T$ values of 1.25 at 4D spacing and 1.30 at 3D spacing. Observed that, in general, cyclic loading caused deflections to approximately double.
Singh, A. Prakash, S. (1971)	Conducted <b>1g model tests</b> on 4-pile groups spaced at 4D. Model piles were 0.5-in-square aluminum tubes, 24-in-long. Conditions of free rotation and no rotation were imposed at the pile heads. The model tank size was 47 by 47 by 47 in deep.	clean sand, $D_r=80\%$ and $\phi=46^\circ$	Determined that cyclic response of the 4-pile group was similar to the individual pile in terms of pile head deflection. However, piles in the group were observed to be more sensitive to changes in moment than the single pile. Restraining the cap from rotation reduced the percentage increase in deflections and moments caused by cyclic loading. Applying a vertical load to the pile group did not effect the lateral behavior.

Table A.1. Continued.

Reference	Lateral Load Test Description	Foundation Soil	Principal Findings
Kim, J.B. Singh, L.P. Brungraber, R.J. (1979)	Conducted <b>full-scale field tests</b> on three groups of fixed-headed 10BP42 piles at 4.8D and 3.6D c/c spacings. Two groups were vertical and one group contained battered piles. The pile cap was constructed on the ground surface, with its soffit in contact with the soil.	Piles were driven to refusal through 40 ft of uniform clay to fractured limestone.	Measured lateral group efficiencies ( $G_e$ ) greater than unity. $G_e$ was determined by comparing the response of a single isolated free-headed pile with an individual fixed-headed pile from a group. Attributed $G_e$ 's greater than 1 to double curvature bending caused by the restraint of the pile cap. They found that as the load increased to the yield load, $G_e$ decreased and approached unity. Determined that cap soil contact can have a significant effect on the resistance to lateral loads. Determined that when more than half of the piles are battered the cap soil contact has very little effect.
Hughes, J.M. Fendall, H.D. Goldsmith, P.R. (1980)	Conducted <b>1 g model tests</b> on two in-line 0.8 by 0.8 in square steel piles with pinned-head connections.	dry sand placed by pluviation and vibra-compaction	Used photogrammetric and radiographic techniques to observe sand movements around driven piles. Observed movement in sand grains up to 6D from pile centerline during driving. Determined that the method of sand placement has a substantial effect on stiffness, ... <i>continued</i> .

Table A.1. Continued.

Reference	Lateral Load Test Description	Foundation Soil	Principal Findings
Hughes, J.M. (1980) <i>continued</i>	<i>continued from previous page</i>		...even if densities are the same. The front pile took more load than the rear, up to a spacing of 13D. Observed that elastic continuum methods were less than adequate in predicting the soil interaction effects that were measured during the experiments.
Matlock, H. Ingram, W.B. Kelley, A.E. Bogard, D. (1980)	Conducted <b>full-scale field tests</b> on 5- and 10-pile circular groups of 6-inch-diameter free-headed pipe piles, spaced at 3.4D and 1.8D, respectively.	soft to very soft clay	Measured static deflections of the 5-pile group (3.4D spacing) were twice the single-pile values, and those for the 10-pile group (1.8D spacing) were 3 times as great. However, variations in measured bending moments were generally less than 10 % and rarely exceeded 20 %. Group effects measured during cyclic loading were substantially reduced from static values.
Holloway, D.M. Moriwaki, Y. Perez, J.Y. (1981)	Conducted <b>full-scale field tests</b> on a 2 by 4 group of 14-inch-diameter fixed-headed timber piles spaced at 2.6D c/c. Piles driven 35 feet into a very dense alluvial outwash deposit.	alluvial soils overlying limestone bedrock	Observed a failure mechanism described as the leading piles “punching” into the soil, while the trailing pile response was altered as the soil mass within the group “tracked” the leading piles. Strain gage data indicated that a significantly larger portion of the shear force was transferred to the leading row of piles compared to the trailing row of piles.

Table A.1. Continued.

Reference	Lateral Load Test Description	Foundation Soil	Principal Findings
Schmidt, H.G. (1981) and Schmidt, H.G. (1985)	Conducted <b>full-scale field tests</b> on bored piles (concrete drilled shafts). Measured the lateral resistance of in-line (pile files) 47-in-diameter bored piles at spacings of 2D, 2.2D and 3D. Shafts were tested free-headed with bore lengths of 28 feet.	uniform medium-dense sand above the water table	Concluded that group action (for pile files) was negligible at spacing of 3D or greater. At spacing less than 3D the leading pile behaves as an isolated pile and the middle and trailing pile behaviors coincide. Minimum $G_e$ 's of 0.75 to 0.8 were measured at a spacing of 2D. Determined that bending moments were generally the same regardless of pile location or pile spacing.
Barton, Y. O. (1984)	Conducted <b>centrifuge tests</b> on groups of 2, 3, and 6 piles at accelerations ranging from 30g to 120g. Measured interaction factors between pairs of piles at various spacings and orientations to direction of loading.	fine sand prepared under water at $D_r=79\%$ and $\phi=43^\circ$	One of the earliest studies of group interaction effects using the centrifuge. Demonstrated that nonlinear pile group response is evident even at small strains. Determined that elastic methods do not accurately model soil non-linearity effects caused by group action, even at small strain strains. Developed interaction factors for pairs of piles in groups of different sizes with different pile spacings.
Cox, W.R. Dixon, D.A. Murphy, B.S. (1984)	Conducted <b>1g model tests</b> on groups of 1-inch-diameter steel tubing inserted to depths ranging from 2 to 8 diameters. Performed tests on single piles and on 3 and 5 pile groups with clear spacings of 0.5, 1, 2, 3, and 5 diameters.	very soft processed clay placed in a 25 in by 25 in by 16 – inch-deep test box $S_u = 0.42$ ksf	Evaluated group efficiencies by examining the response of piles in side-by-side and in-line arrangements. Determined that group effects were negligible when side-by-side spacing exceeds 3D and in-line spacing exceeds 8D.

Table A.1. Continued.

Reference	Lateral Load Test Description	Foundation Soil	Principal Findings
Selby, A.G. Poulos, H.G. (1984)	Conducted <b>1g model tests</b> on pile groups ranging in size from 2 to 9 piles at spacings ranging from 3D to 5D. Model piles were 0.35-in-diameter, 11.4-in-long aluminum tubes. Pile heads were constrained by a stiff steel segmental cap. Test tank size was 23.6 by 17.7 by 27.6 in deep.	uniform sand, rained into the tank around pre-assembled pile groups	Measured significantly higher moments and shears in leading piles compared to central and trailing piles. They called this effect “shielding”. Elastic and continuum analytical methods were unsuccessful in predicting the uneven spread of moments and shears among the piles because these methods did not account for the “shielding” effects.
Baguelin, F. Jezequel, J.F. Meimon, Y. (1985) and Meimon, Y. Baguelin, F. Jezequel, J.F. (1986)	Conducted <b>full-scale field tests</b> on a 3 x 2 pile group spaced at 3D in the direction of load and 2D normal to load direction. Piles consisted of boxed I-beams, 11.2 by 10.6 in, driven 24.6 ft. Pin-headed connections were used.	1 m of CH over 13 ft of CL over 13 ft of SM	Measured increased group effect with load, characterized by differences in behavior between rows. Determined that shear and moments were nearly constant between piles in a given row. However, measured higher shear forces and moments in the leading row compared to the trailing row. Determined that cyclic loading tended to equalize the interaction factors between rows.

Table A.1. Continued.

Reference	Lateral Load Test Description	Foundation Soil	Principal Findings
Brown, D.A. Reese, L.R. (1985) and Brown, D.A. Reese, L.R. O'Neill, M.W. (1987)	Conducted <b>full-scale field tests</b> on a 3 x 3 group of steel pipe piles spaced at 3D c/c. A loading frame was used that provided moment-free connections at each pile head.	stiff overconsolidated clay, $S_u = 1.2$ to 1.7 ksf, piles were driven close-ended to a depth of 43 feet	Measurements indicated that load transferred to the piles was predominately a function of the row-to-row position of the pile rather than the position of the pile normal to the direction of load. Large proportions of shear were measured in the leading row, with successively less shear distributed to the middle and back rows. Observed that elasticity based approaches do not adequately address the reduction of soil resistance caused by soil interaction effects.
Clark, J.I. Mckeown, S. Lester, W.B. Eibner L.J. (1985)	Conducted <b>full-scale field tests</b> on small free-headed groups (2 to 3 piles) of 3-ft to 5-ft-dia. drilled shafts. Testing conducted during construction of the Olympic Oval Facility in Calgary.	23 ft of compact sand overlying firm ablation till	Determined that measured results did not agree with calculated results for single piles. Attributed the discrepancy to group effects and consequently reduced the single pile soil stiffness by 24 %.
Sarsby, R.W. (1985)	Conducted <b>1g model tests</b> on groups containing 2 to 4 0.24-in-dia mild steel bars spaced at 2D to 17D. The groups were oriented in a single line of piles and were tested in a free-headed condition. Piles were driven through sand placed in a steel tank of size 31.5 by 35.5 by 35.5 in deep.	poorly graded, dry, medium-fine sand, $\phi = 38^\circ$ , placed and compacted in layers	Determined that group efficiency does not markedly change with deformation. Observed that pile efficiency factors determined using Poulos's interaction factors agreed with measured results for small pile groups, but was conservative for large groups. ...continued

Table A.1. Continued.

Reference	Lateral Load Test Description	Foundation Soil	Principal Findings
Sarsby, R.W. (1985) <i>continued</i>	<i>continued from previous page</i>		...Concluded that the load–deflection curve could accurately be described by a simple power law.
Morrison, C. Reese, L.C. (1986) and Brown, D.A. Morrison, C. Reese, L.R. (1988)	Conducted <b>full-scale field tests</b> on a 3 x 3 group of steel pipe piles spaced at 3D c/c. A loading frame was used that provided moment-free connections at each pile head. (This test setup was previously used in the Brown et al., 1987 study.)	In situ soils were removed and med. dense sand was placed and compacted around the piles at a $D_r$ of 50 %, $\phi=38.5^\circ$ .	Defined the term “shadowing”, in which the soil resistance of a pile in a trailing row is reduced because of the presence of the pile ahead of it. Developed the concept of using a p-multiplier to modify the single pile p-y curve to obtain a group pile p-y curve. Suggested using p-multipliers of 0.8, 0.4, and 0.3 for the leading, middle, and back rows, respectively of pile groups spaced at 3D c/c.
Franke, E. (1988)	Conducted <b>1g model tests</b> on 1 x 3 and 3 x 1 groups with moveable heads. Test piles were 1.6-in-diameter and were grouped in spacings ranging from 2D to 8D.	fine sand rained around the pre-installed piles at different relative densities	Determined that group interaction effects occur when pile spacing in the direction of load is less than 6D and/or the spacing perpendicular to load direction is less than 3D. Developed normalized interaction factors as a function of pile spacing and sand density for rigid and flexible piles.
Blaney, G.W. O’Neill, M.W. (1989)	Conducted full-scale field tests on a 3 x 3 group of 10.75-in-dia steel piles constrained by a rigid concrete cap. Dynamic loading tests were performed using a linear inertia mass vibrator attached to the top of the pile cap, which was constructed approximately 2.6 feet above the ground surface.	stiff overconsolidated clay, $S_u = 1.2$ to 1.7 ksf, piles were driven close-ended to a depth of 43 feet	Concluded that the response of the system was largely controlled by the superstructure response (applied dynamic loading). Determined that the stiffness of individual group piles were approximately 70% of the stiffness of a comparable single pile.

Table A.1. Continued.

Reference	Lateral Load Test Description	Foundation Soil	Principal Findings
Lieng, J.T. (1989)	Conducted <b>1g model tests</b> on 2 vertical piles at various spacings. Piles were 5.9-in-dia., 102-in-long, and 0.2-in-thick aluminum pipes.	dry loose sand was rained into a 13 by 13 by 10 ft tank	Determined that group efficiency is inversely related to magnitude of applied load. Observed that rear piles develop resistance in deeper layers than the front piles because the shear resistance in the upper layers of soil around the rear piles is reduced due to shadowing effects. Did not detect any pile-soil-pile interaction between piles in a given row for spacings greater than 3D.
Ochoa, M. O'Neill, M.W. (1989)	Conducted <b>full-scale field tests</b> on the same 3 x 3 group of 10.75-inch diameter piles that were used in Brown's 1988 study.	In situ soils were removed and med. dense sand was placed and compacted around the piles at a $D_r$ of 50 %.	Developed lateral interaction $\alpha$ -factors, which relate to the stretching of the deflection portion of the pile resistance curve. The $\alpha$ factors cannot be used directly to analyze individual piles because they are not explicitly applied to p-y curves. The factors were found to increase with increasing load magnitude and decrease with increasing number of load cycles.
Shibata, T. Yashima, A. Kimura, M. (1989)	Conducted <b>1g model tests</b> on 31.5-in-long, 0.87-in-diameter aluminum and chloridized-vinyl pipes. Universal joints were attached to pile heads to provide free rotation of pile tops. Piles were installed in the test tank during soil preparation by the "boiling technique". Pile groups ranged in size from 2 to 16 piles at spacings ranging from 1.8D to 9.1D.	Uniform sand was "boiled" into test tank by pumping water with an upward gradient through the bottom of the tank. $D_r=20\%$ .	Compared measured test results to theoretical predictions using the method developed by Randolph (1981) for flexible free-headed piles. Good agreement was obtained between predicted and measured values of group efficiency, with a maximum discrepancy of 30 %.

Table A.1. Continued.

Reference	Lateral Load Test Description	Foundation Soil	Principal Findings
Liu, J.L. (1991)	Conducted <b>1g model tests</b> on 28 sets of bored pile groups with different pile spacings, diameters, geometric arrangements, and lengths.	silt – (no additional information provided on soil characteristics or test details)	Concluded: 1) front row piles take the largest share of applied lateral load, 2) pile group interaction varies with pile spacing and number of piles in the direction of load, 3) partial restraint of pile head results in redistribution and decrease of bending moments in pile head and shaft, and 4) cap side resistance and bottom friction increase the overall lateral bearing capacity.
Zhang, L. Hu, T. (1991)	Conducted <b>centrifuge tests</b> on piles and pile groups. Placed soil and installed piles at 1g, loaded piles at 50g.	soil 1: uniform silty clay, soil 2: stratified deposit of silty clay over fine sand	Studied the effects of residual stresses in piles and the variation of stresses between piles during static and cyclic loading. Negligible residual stresses were measured in the clay, while substantial residual stresses were measured in the sand and stratified soil layers.
Adachi, T. Kimura, M. Kobayashi, H. Morimoto, A. (1994)	Conducted <b>centrifuge tests</b> on two aluminum pipe piles with pinned heads at 40g acceleration. The pile spacing and skew angle were varied to investigate group effects.	dry sand at a relative density of about 90 %	Concluded that for a 2-pile in-line group, the front pile takes a larger portion of shear than the rear pile. Developed interaction factors for various pile spacings and skew angles.

Table A.1. Continued.

Reference	Lateral Load Test Description	Foundation Soil	Principal Findings
Kotthaus, M. Grundhoff, T. Jessberger, H.L. (1994)	Performed <b>centrifuge tests</b> on three aluminum tubes with fixed-heads at 50g acceleration. Pile row spacings of 3D and 4D were used. Soil was placed after installing the piles, at 1g. Tank size was 2.8 by 1.4 by 2.6 ft deep.	fine-grained sand placed by pluvial deposition at $D_r = 98\%$	Determined that group efficiency effects varied as a function of pile displacement, up to a limiting displacement of approximately 10 % of the pile diameter, for 3D and 4D row spacings.
McVay, M. Bloomquist, D. Vanderlinde, D. Clausen, J. (1994) and McVay, M. Casper, R. Shang, T.I. (1995)	Conducted <b>centrifuge tests</b> on 3 x 3 groups of free-headed piles at 3D and 5D center to center spacing. Piles were driven and laterally loaded in flight at 45g acceleration.	medium loose ( $D_r=33\%$ , $\phi=34^\circ$ ) and medium dense ( $D_r=55\%$ , $\phi=30^\circ$ ) sand, classified as SP	COM624P was used to back-calculate p-multipliers for each pile row. The group efficiency ( $G_e$ ) was independent of soil density and was only a function of pile group geometry. $G_e$ at 3D spacing was 0.74 and $G_e$ at 5D was 0.94.
Chen, L.T. Poulos, H.G. (1996)	Conducted <b>1g model tests</b> on pile groups using 1-in-dia. aluminum tubes, 3.28-ft-long. Three types of groups geometries were tested: in-line rows, side-by-side rows, and in square (box) arrangements. Tests were conducted on free-headed and fixed-headed groups at spacings ranging from 2.5D to 7.5D.	calcareous sand rained into an aluminum tank of dimensions 19.5 by 16.0 by 27.6 in deep	Evaluated group effects based on the position of a pile in a group, pile spacing, the number of piles, and the head fixity. Determined that a rigid pile cap reduces the positive bending moment and causes a relatively large negative bending moment in the upper portion of the pile. Evaluated group efficiencies based on maximum positive bending moments and compared experimental results to those calculated using the boundary element computer program PALLAS.

Table A.1. Continued.

Reference	Lateral Load Test Description	Foundation Soil	Principal Findings
Rao, S.N. Ramakrishna, V.G. Raju, G.B. (1996)	Conducted <b>1g model tests</b> using 21.5-mm-diameter, 1,000-mm-long, mild steel pipe piles. Two and three pile groups were tested at spacings ranging from 3D to 6D.	marine clay, LL=82 % and PL=32 %	Experimentally determined that pile group capacity depends on the spacing and arrangement of piles. Determined that for spacings greater than 6D in the direction of load, or 3D normal to load direction, $G_e$ approached 1. Performed a simplified plane strain 3D finite element analysis and tabulated comparisons between measured and calculated group efficiencies.
Gandhi, S.R. Selvam, S. (1997)	Conducted <b>1g model tests</b> on groups with 2 to 9 piles in 21 different configurations. The piles consisted of 0.72-in-O.D. aluminum pipes installed at c/c spacings varying from 4D to 12D.	Clean fine to medium sand placed at 60 % relative density in a 2.3 by 2.3 by 2.0 ft deep test tank.	Developed relationships for nondimensional interaction load factors in terms of pile spacing and relative stiffness, $T$ . Where, $T = (EI/n_p)^{1/5}$ . Determined the optimum pile spacing (in the direction of load) was two times $T$ , for maximum group efficiency.
Rollins, K.M. Weaver, T.J. (1997)	Conducted <b>full-scale field tests</b> on a 3 x 3 pile group at 3D spacing. The piles were 12-in-I.D. closed-end steel pipes driven to a depth of 30 ft. Pinned-headed connections were used to apply the test loads.	cohesive soils classified as ML, CL-ML, or CL with an avg. $S_u$ of 0.5 to 1.0 ksf	Measured group efficiency factors for individual pile rows. Presented design curves for p-multipliers as a function of pile spacing for leading row and trailing row piles. Did not observe any consistent trends in the load distribution among piles in the same row.

Table A.1. Concluded.

Reference	Lateral Load Test Description	Foundation Soil	Principal Findings
Ruesta, P.F. Townsend, F.C. (1997)	Conducted <b>full-scale field tests</b> (Roosevelt Bridge Project) on 2 groups (one fixed- and one free-headed) of 16 prestressed concrete piles spaced at 3D. Piles were jetted 25 ft and driven 29 ft.	loose fine sand to 15 ft depth, $D_r=30\%$ and $\phi=32^\circ$ , underlain by v. dense cemented sand	Measured p-multipliers of 0.8, 0.7, 0.3, and 0.3 from leading to trailing rows for the free-headed test pile group. Fixed-head tests gave approximately the same results. The pile group load-deflection efficiency was 80 %. The variation of bending moments between different rows was less than 15 %.
McVay, M. Zhang, L. Molnit, T. Lai, P. (1998)	Conducted <b>centrifuge tests</b> on 3 x 3 through 7 x 3 groups of fixed-headed piles at 3D c/c spacings. Piles were pushed and laterally loaded in flight at 45g acceleration.	medium loose ( $D_r=36\%$ , $\phi=34^\circ$ ) and medium dense ( $D_r=55\%$ , $\phi=37^\circ$ ) sand Classified as SP	Concluded that an individual pile row's contribution to the group's lateral resistance did not change with size of group, only with its row position. Observed that position of pile within a row had no significant effect on its lateral resistance. Provided p-multipliers for laterally loaded pile groups with 3 to seven rows of piles spaced at 3D. Concluded that Brown et al.'s (1988) p-multiplier approach is accurate for matching the total group load and individual row distributions.

Table A.2. Summary of pile group analytical studies.

Reference	Method of Analysis	Principal Findings
Kim, J.B. (1969)	analytical approach	Developed a procedure and computer program that incorporate group effects for closely spaced piles with the equivalent cantilever method of analyzing single piles. Group effects are accounted for by modifying the coefficient of subgrade reaction based on pile spacing and pile location within the group.
Poulos, H.G. (1971a) and Poulos, H.G. (1971b)	elasticity theory	Modeled pile-soil interactions using elastic continuum methods that consider the soil to act as a 3-D, linearly elastic, homogeneous, isotropic, semi-infinite medium. Used Mindlin's equations to develop factors that account for additional displacements ( $\alpha_p$ ) and rotations ( $\alpha_\theta$ ) caused by interactions from adjacent piles. Developed, in chart form, interaction factors for free-head and fixed-head piles subjected to horizontal loads and moments applied at the ground surface.
Focht, J.A. Koch, K.J. (1973)	hybrid method	Developed a hybrid procedure that uses p-y curves to model pile-soil interaction and Mindlin's equations with elasticity based $\alpha$ -factors to approximate the group effects of pile-soil-pile-interaction. (The original hybrid method for analyzing pile groups.) Presents a procedure for including interaction effects of closely spaced piles by applying y-multipliers to single pile p-y curves. Recommend using a soil modulus, $E_s$ , that corresponds to low stress levels in the soil. They recommend a value between the initial tangent modulus and 25 % of the ultimate stress.
O'Neill, M.W. Ghazzaly, O.I. Ha, H.B. (1977)	hybrid method	Presented a method for analyzing pile groups using a hybrid-type of analysis. Deviated from the Focht-Koch procedure by modifying unit-load-transfer curves individually to account for stresses induced by adjacent piles. The method is based on a discrete element formulation for pile-soil load transfer behavior coupled with an elastic half-space representation of the pile-soil-pile interaction effects.

Table A.2. Continued.

Reference	Method of Analysis	Principal Findings
Banerjee, P.K. Davies, T.G. (1980)	elastic continuum with boundary element methods	Extended general boundary element methods (using reciprocal work theory) to incorporate elasto-plasticity models through an initial stress, an initial strain, and a modified body force algorithm. Demonstrated that group response is dependent on pile spacing and geometric arrangement.
Desai, C.S. Kuppusamy, T. Alameddine, A.R. (1980)	2-D finite element study	Determined parametrically that the relative stiffness of cap, pile, and soil medium have a considerable influence on the distribution of load in piles within a group. Determined that for stresses in the linear range, this method yields results similar to other numerical procedures such as Hrennikoff's approach.
Randolph, M.F. (1981)	finite element parametric study with elasticity approach	Performed parametric studies using finite element methods and Poulos's elasticity approach to develop algebraic equations for estimating the lateral response of single piles. Treated the soil as an elastic continuum with either a constant or linearly varying modulus. Extended the analysis to consider pile groups by developing expressions for interaction factors for closely spaced piles. The solutions are simpler than previous continuum methods because they are independent of the embedment length of the pile. Randolph reports that only in rare cases will the length of the pile be a factor.
Hariharan, M. Kumarasamy, K. (1982)	analytical approach	The authors address group effects by applying two multipliers to the p-y curve for a single pile, one for the load and the other for the displacement. The multipliers are determined by normalizing the stresses and deformations in a horizontal layer due to movement of the piles (equations determined using elastic continuum methods). Average multipliers are used for all the piles in a group, rather than different multipliers for different piles. The authors suggest this assumption is sufficiently accurate for design purposes.

Table A.2. Continued.

Reference	Method of Analysis	Principal Findings
Tamura, A. Ozawa, Y. Sunami, S. Murakami, S. (1982)	3-D finite element study	Performed 3-D finite element analyses using the hyperbolic model to represent the stress-strain characteristics of the soil. Performed parametric studies to evaluate group effects related to pile spacing and quantity of piles. Determined that pile group effects increase as the number of piles in the direction of load application increases and as pile spacing decreases. Observed that the inner piles took a greater portion of load and had larger group effects than the outer piles.
O'Neill, M.W. (1983) Brown, D.A. Reese, L.C. (1985) and Reese, L.C. Wang, S.T. (1996)	empirical analytical approach	Developed the p-multiplier approach to account for pile group shadowing effects. The p-y curve is softened or weakened by multiplying the soil resistance, p, by a reduction factor, $f_m$ . This method is combined with a structural matrix analysis package in the computer program GROUP.
Bogard, D. Matlock, H. (1983)	analytical approach - modified unit load transfer procedure	Developed a method for constructing nonlinear resistance curves for use with a Winkler-type soil model. Pile group behavior was modeled by replacing the group with an imaginary or equivalent pile and the soil behavior was softened by applying a group efficiency factor. They concluded that the deflection of piles in a group is related to both the deflection of the piles acting individually and the deflection of the large equivalent pile. Deflections are determined by combining the nonlinear component from group-pile interaction with the nonlinear component from individual-pile deflection within the field of global soil deformation.
Reese, L.C. Wright, S.G. Aurora, R.P. (1984)	hybrid method	Evaluated the use of hybrid approaches for analyzing the lateral response of pile groups. Presented a modification to the Focht and Koch (1973) hybrid approach in which the elastic deflections used in the group deflection equations are estimated from the results of p-y analyses performed at load levels where load-deflection behavior is linear.

Table A.2. Continued.

Reference	Method of Analysis	Principal Findings
Sogge, R.L. (1984)	2-D finite element study	Presented the results of 2-D finite element analyses using a straightforward beam-element program that unified the soil model with the structural model. Demonstrated the suitability of using the coefficient of subgrade reaction to represent the soil strength.
Dunnivant, T.W. O'Neill, M.W. (1986) and O'Neill, M.W. Reese, L.C. Cox, W.R. (1990)	empirical analytical approach	Used experimental studies to develop a stiffness distribution model, which is sometimes referred to as the $\beta$ method. Presented p-y reduction factors (p-multipliers) for side-by-side, in-line, and skewed arrangements of piles at various spacings. The method provides a means to account for shadowing effects in which the leading piles carry more load than the trailing piles.
Leung, C.F. Chow, Y.K. (1987)	semi-theoretical hybrid approach	Developed a hybrid method in which the individual pile response is modeled by the conventional p-y approach while group interaction is based on flexibility coefficients obtained from Mindlin's solution.
Najjar, Y.M. Zaman, M.M. (1988)	3-D finite element study	Performed nonlinear 3-D finite element analyses to investigate the effects of loading sequence and soil nonlinearity on the deformation behavior of a pile group. The behavior of the pile and cap was assumed linear. A nonlinear constitutive model was used for the soil. Observed that loading sequence and soil nonlinearity can significantly affect the lateral and axial response of pile groups. Developed a compute code for post-processing results and for plotting contours of the stress and displacement components of the pile-cap-soil system.
Lieng, J.T. (1989)	analytical approach	Developed a plasticity approach based on the concepts of effective stress analysis. The approach is similar to Janbu's tangent modulus method for calculating the settlement of a strip footing. Developed an expression for calculating the minimum pile spacing at which shadow effects approach zero.

Table A.2. Continued.

Reference	Method of Analysis	Principal Findings
Novak, M. Janes, M. (1989)	analytical approach	Developed closed-form expressions for evaluating group stiffness and damping. These expressions can be applied to estimate group response under small displacements, as a result of static and dynamic lateral loads.
Ochoa, M. O'Neill, M.W. (1989)	elasticity theory	Presented a method for analyzing pile groups using elasticity theory with experimentally determined interaction factors.
Brown, D.A. Shie, C.F. (1991)	3-D finite element study	Performed a detailed parametric study using a 3-D finite element model to evaluate the combined effects of superposition of elastic strains and shadowing. Two constitutive models for soil were used; an elastic-plastic constant yield strength (Von Mises envelope) for undrained loading of saturated clay, and an extended Drucker-Prager model with a nonassociated flow rule was used for sand. Developed recommendations for modifying p-y curves (as a function of pile spacing) using p- and y-multipliers. Observed that these multipliers vary as a function of depth and soil type, but the variations are small and do not warrant consideration in design.
Clemente, J.L. Sayed, S.M. (1991)	semi-empirical analytical approach	Developed a semi-empirical expression for estimating group response using elasticity theory. Presented expressions and charts for estimating the radial and circumferential hoop strain components around a pile. Developed a procedure to estimate pile group efficiencies using these radial strain components.

Table A.2. Continued.

Reference	Method of Analysis	Principal Findings
Iyer, P. Sam, C. (1991)	elasticity theory	Developed a method for estimating the stresses in a 3-pile cap using 3-D elasticity solutions expressed in terms of the Galerkin vector and double-Fourier series. The cap was modeled as a thick rectangular block with patch loadings on the top and bottom faces. Concluded that this method of structural analysis was more accurate than the truss analogy and beam methods.
Garassino, A.L. (1994)	hybrid method	The author presents an iterative elasticity approach for representing group behavior in which a p-multiplier is used to scale down the ultimate resistance and a y-multiplier is used to modify the deflection using Poulos's elastic theory. The author presented a general review of various other methods including finite element and subgrade reaction approaches.
Ooi, P.S. Duncan, J.M. (1994)	hybrid method - group amplification procedure	Performed a parametric study of pile group response using the Focht-Koch procedure. Developed a method for estimating the increased deflections and bending moments in laterally loaded piles and drilled shafts caused by group interaction effects. Developed design charts and equations for determining deflections and bending moments of closely spaced piles.
Narasimha, Rao Ramakrishna, V.G. (1995)	2-D finite element study	Analyzed 2-pile and 3-pile groups with pile spacing varying from 3D to 8D and with cap thickness varying from 0.12 in to 0.60 in. (The pile caps were not in contact with the soil.) Determined that the lateral resistance of a pile group depends not only on the spacing between piles but also on the thickness of the pile cap. The pile cap deforms as a flexible body when its thickness is small and it deforms as a rigid body at larger thickness.

Table A.2. Concluded.

Reference	Method of Analysis	Principal Findings
Ashour, M. Pilling, P. Norris, G. Perez, H. (1996)	analytical approach	Developed an analytical approach (incorporated into the computer program SWSG) known as the strain wedge model to evaluate the response of piles and pile groups. The model relates 1-D beam on elastic foundation analysis to 3-D soil pile interaction response, which is based on the deformation of soil within a plastic wedge in front of the pile. Plane stress conditions are assumed within the wedge and group effects are quantified by considering the overlap of passive wedges and accompanying strains.
Rao, S.N. Ramakrishna, V.G. Raju, G.B. (1996)	2-D finite element study	Performed simplified plain strain finite element analyses to evaluate group efficiencies for various pile spacings and geometric arrangements. Compared calculated results with those obtained from 1g model tests.
Gandhi, S.R. Selvam, S. (1997)	analytical approach	Present a nondimensional method for predicting pile response based on a power function relationship. Multiplication factors, determined from 1g model tests, were used to model group behavior.

**APPENDIX B**

**DETAILS OF LOAD TEST FACILITY AND COST OF  
CONSTRUCTION**

Table B.1. Pile driving system specifications.

<b>Pile hammer: ICE model 30S double-acting diesel hammer</b>	
rated energy	22,500 ft-lb
minimum energy	9,000 ft-lb
stroke at rated energy	7.5 ft
maximum attainable stroke	7.67 ft
speed	44 to 67 blows per minute
hammer weight	6,250 lb
ram weight	3,000 lb
anvil weight	560 lb
typical operating weight with cap	7,340 lb
<b>Nylon pile driving cushion</b>	
thickness	1.5 in
stiffness	$85 \times 10^6$ lb/in
elastic modulus	$35 \times 10^4$ psi
<b>Aluminum pile driving cushion</b>	
thickness	0.5 in
stiffness	$69 \times 10^6$ lb/in
elastic modulus	$10 \times 10^6$ psi

Data furnished by Drive-Con, Inc., Jessup, Maryland.

Table B.2. Summary of pile driving data.

Pile number	Initial pile length <sup>1</sup> (ft)	Pile head elevation <sup>2</sup> (ft)	Pile tip elevation (ft)	Pile head cutoff elev. <sup>3</sup> (ft)
P1	20.0	100.77	80.77	97.20
P2	20.0	98.49	78.49	97.20
P3	20.0	98.52	78.52	97.20
P4	20.0	99.96	79.96	97.20
P5	20.0	98.35	78.35	96.45
P6	20.0	98.45	78.45	96.45
P7	20.0	98.45	78.45	96.45
P8	20.0	98.47	78.47	96.45
P9	20.0	99.05	79.05	99.05
P10	20.0	98.79	78.79	98.79
P11	11.3	98.22	86.92	97.20
P12	11.3	98.12	86.87	97.20
P13	11.3	98.20	86.89	97.20
P14	11.3	98.09	86.87	97.20

## Notes:

1. As-delivered length of HP 10x42, ASTM A-36 carbon steel pile sections.
2. Elevation measurements are based on a project datum of 100.00. Average ground surface elevation = 97.80.
3. Excess pile stickup was cut off after driving to provide 0.3 feet of clearance between the pile and the top surface of the pile cap. The final surface elevation was 97.50 for the two 36-inch-deep caps and 96.75 for the 18-inch-deep cap.

Table B.3. Potentiometer standard specifications.

<b>Deflection instrument</b>	<b>Longfellow linear transducer</b>	<b>Celesco cable-extension transducer</b>
Model Number	SLF-S-150-D-1	PT101-0010-111-1110
Sensor resistance	9000 $\Omega$	500
Linearity	0.10 % full scale	0.15 % full scale
Excitation voltage	10 V	10 V
Full scale rating	6 in	10 in

Table B.4. Instrument calibration data.

Instrument number	Model	Serial number or type	Block number	Channel number	Board number <sup>1</sup>	Calibration slope (in/volt)	Module AIM3A serial No.
1 – SLF	150-D-1	H84, 8341	16	0	5	-0.5948	0582607
2 - SLF	150-D-1	H84, 8341	--	--	--	-0.5956	--
3 – SLF	150-D-1	H84, 8341	--	--	--	-0.5948	--
4 – SLF	150-D-1	H84, 8341	17	1	5	-0.5953	0582607
5 – SLF	150-D-1	H84, 8341	18	2	5	-0.6003	0582607
6 – SLF	150-D-1	H84, 8341	19	3	5	-0.5954	0582607
7 – SLF	150-D-1	H84, 8341	--	--	--	-0.5950	--
8 – SLF	150-D-1	H84, 8341	--	--	--	-0.5952	--
9 – SLF	150-D-1	H84, 8341	--	--	--	-0.5947	--
10 - Celesco	PT 101	A40564	5	0	3	1.0571	0568533
11- Celesco	PT 101	A55963	6	1	3	1.0597	0568533
12 - Celesco	PT 101	A40574	11	2	3	2.1253	0568533
13 - Celesco	PT 101	A40571	12	3	3	2.1208	0568533
14 - Celesco	PT 101	A55964	10	7	2	1.06142	0568531
15 - Celesco	PT 101	A55966	15	8	2	1.05767	0568531
16 - Celesco	PT 101	F0857898	1	0	2	1.0958	0568531
17- Celesco	PT 101	F0857894	2	1	2	1.0829	0568531
18 - Celesco	PT 101	F0857897	3	2	2	1.0865	0568531
19 - Celesco	PT 101	F0857893	4	3	2	1.0870	0568531
20 - Celesco	PT 101	F085796	7	4	2	1.0830	0568531
21 - Celesco	PT 101	F085795	8	5	2	1.0946	0568531
Load cell	200 kip	VPI – 02	13	0	4	11,124.9 b = 0.00232	0582608
Time block	sec	--	14	--	--	--	--

- Notes:
1. Interface channel number = board number – 1.
  2. System module AMM2 in slot No. 1 of Keithley 500A system.
  3. Calibrated with Keithley 10 V power supply and 2 kHz low-pass filter.
  4. Some instruments listed in the table were not used in the first series of tests.

Table B.5. Cost of equipment and materials.

244 ft of HP 10x42 piles	\$8,300
Pile driving and transporting services – donated, Coalfield Services, Inc.	5,000
VDOT # 57 stone (64 tons)	460
Limestone sand (6 tons)	90
Crusher run gravel (32 tons)	200
4,000 psi ready mix concrete (13 cy)	1,000
Wood	400
Rebar	400
Structural nuts, bolts, and washers	300
Steel bars, plates, etc	350
Miscellaneous fittings, angles, nuts, bolts, paint, tarps, etc.	1,250
Hand tools	350
1987 Dodge Caravan – donated, anonymous donor	2,500
Tent shelter	1,700
Enerpac 200 ton double acting ram	4,000
Enerpac PEM3405 hydraulic pump – borrowed, VPI	0
Honda generator (1600 watt) – borrowed, VPI	0
Northstar generator (5000 watt)	1,000
Gateway 2000 personal computer – donated, VPI	500
Keithley 500A data collection system – borrowed, VPI	0
Celsco transducers (6)	2,200
Celesco and Longfellow transducers (6 each) – borrowed, VPI	0
Strain gauges for 200 kip load cell (8), terminal strips, elect. cable	200
Wacker BS60Y compactor and Troxler nuclear gage – borrowed, VPI	0
Bobcat front-end loader	0
Miscellaneous backhoe services (approx. 25 hours donated by VPI)	0
Machine shop labor (welding, milling, and lathe work)	2,700
Wheel barrow	60
Concrete epoxy	120
Miscellaneous supplies	1,000
Total:	\$34,080

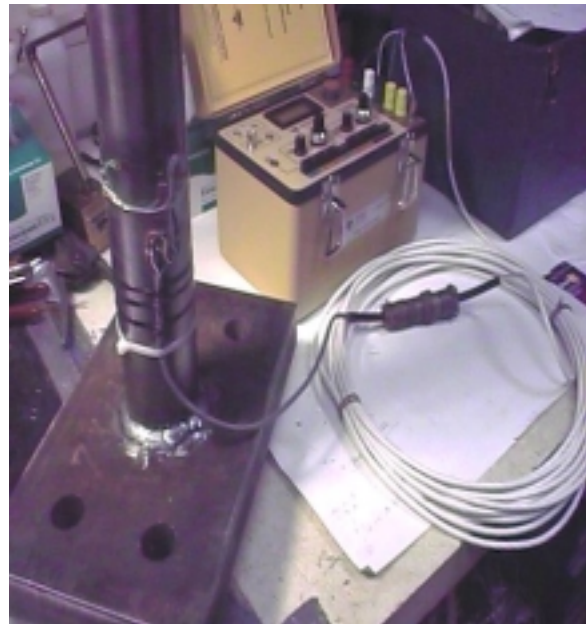
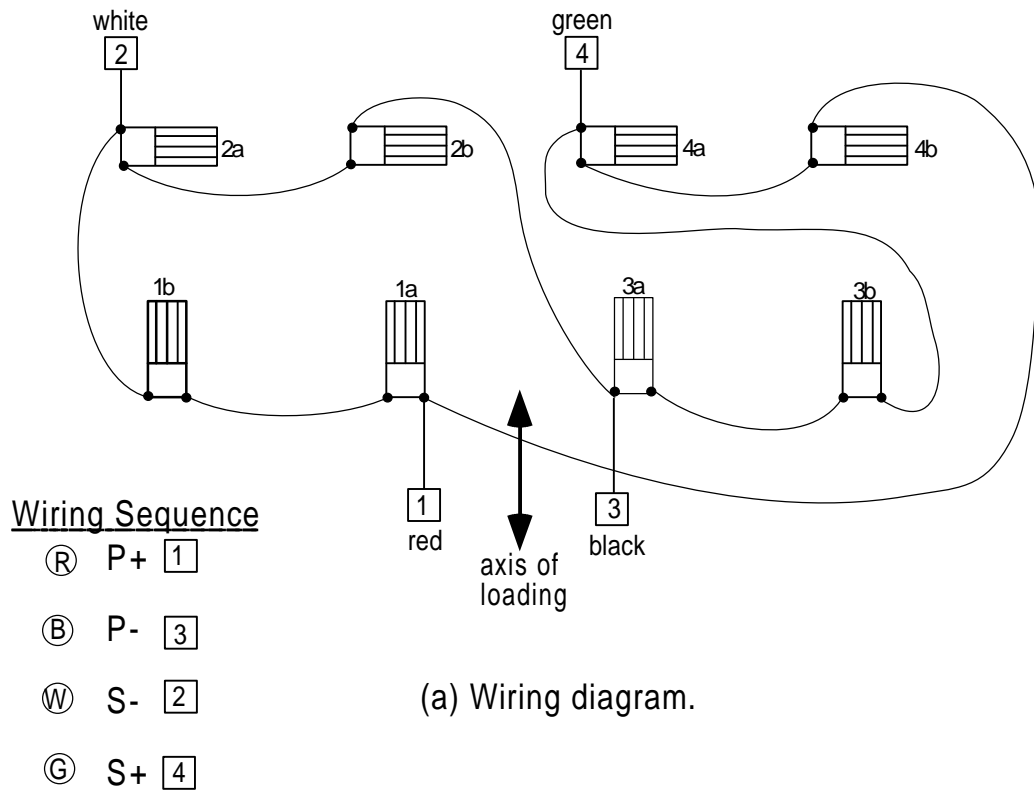
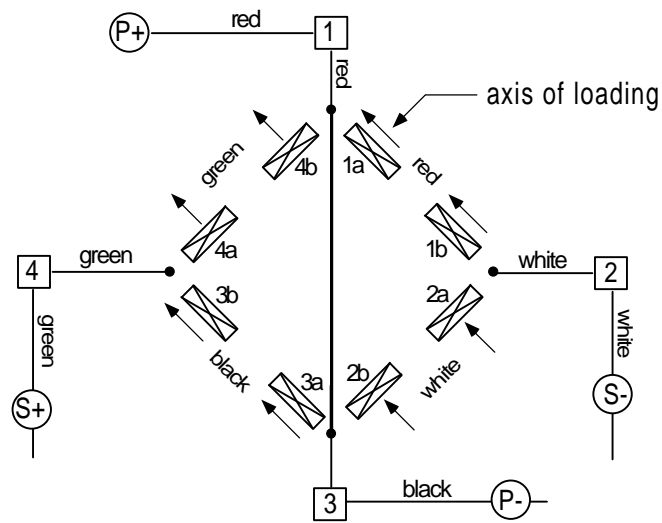


Figure B.1. Building a 200 kip load cell using  $\frac{1}{4}$ -inch strain gauges connected in a Wheatstone full-bridge circuit.



(a) Wiring diagram.



(b) Wheatstone bridge diagram.

Figure B.2. Load cell strain gauge circuit for measuring load.

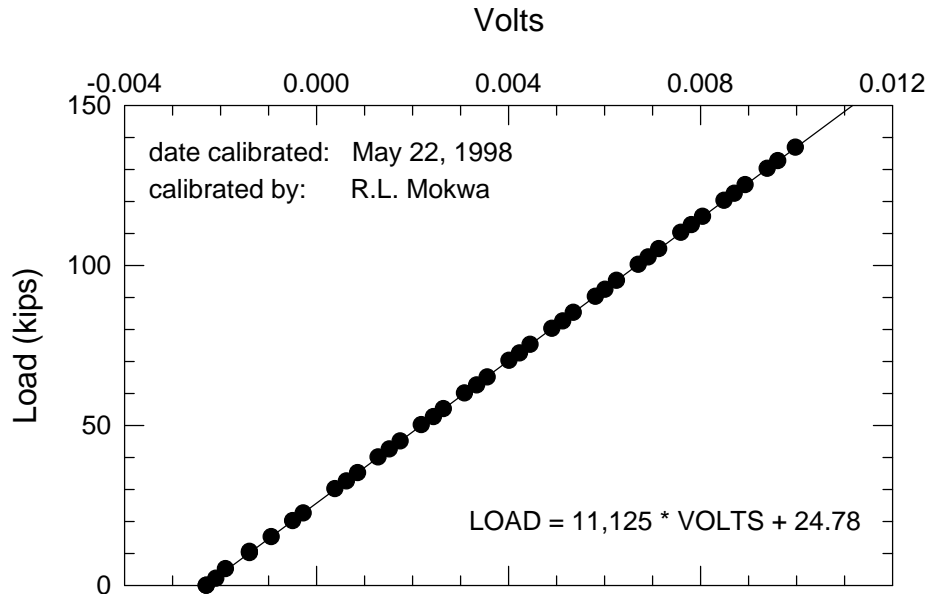


(a) 150 kip load cell.

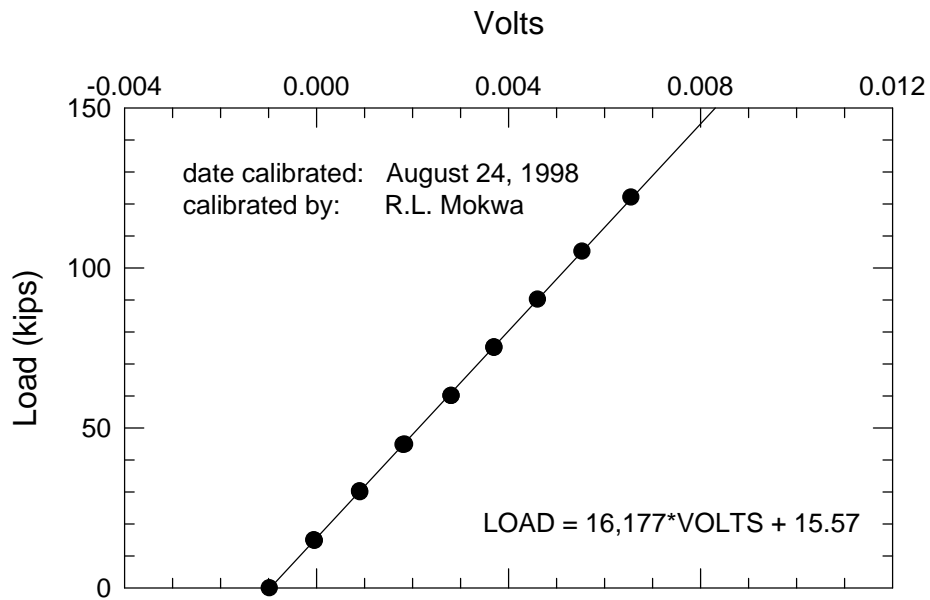


(b) Load test in progress at north pile.

Figure B.3. Single pile test setup.



(a) 200 kip load cell.



(b) 150 kip load cell.

Figure B.4. Calibration curves for load cells.

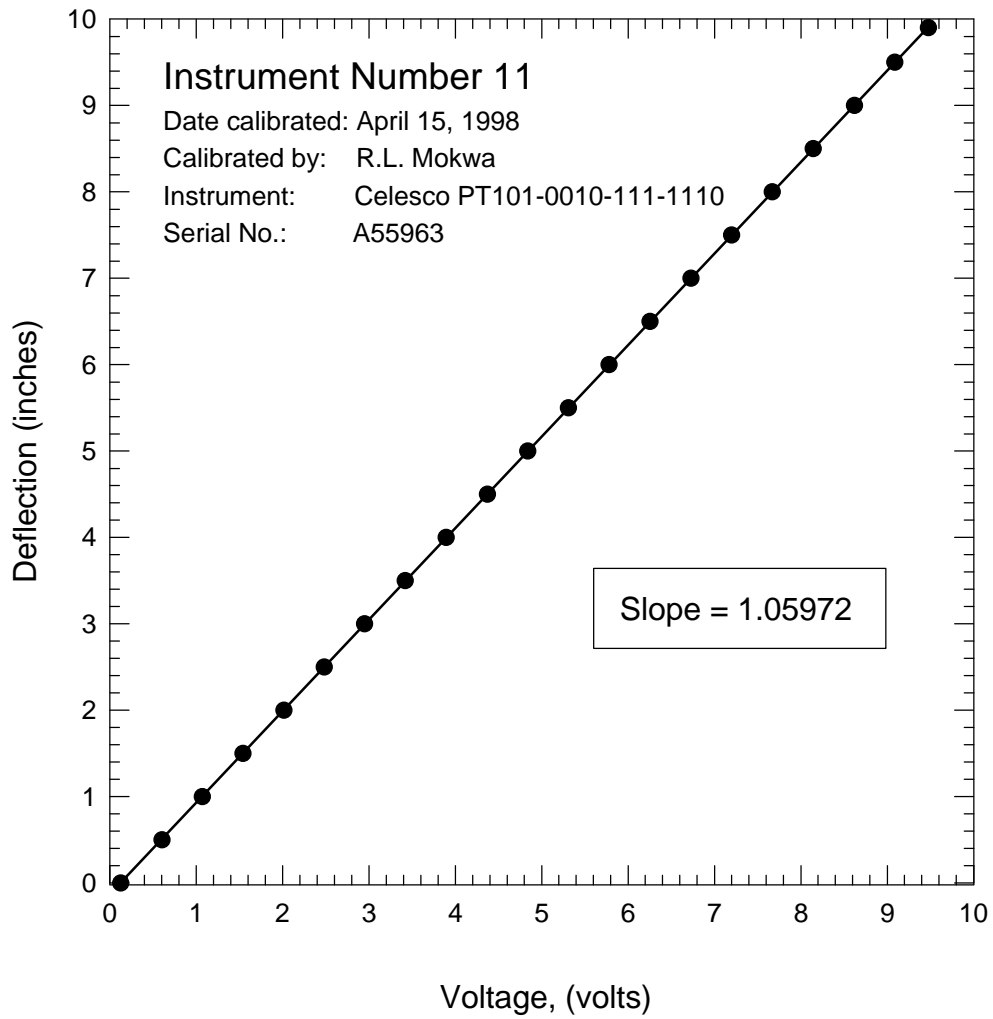


Figure B.5. Calibration curve for deflection transducer No. 11.

**APPENDIX C**  
**SOIL BORING LOGS**



The Charles Edward Via, Jr. Department of Civil Engineering	<b>BORING NUMBER</b> <b>BH-1</b>	<b>SHEET 1 OF 1</b>
<b>SOIL BORING LOG</b>		

PROJECT: Laterally Loaded Pile Cap Research LOCATION: Kentland Farms Site  
 ELEVATION: 98.92 ft DRILLING CONTRACTOR: Va Tech Geotechnical Department, Blacksburg, VA  
 DRILLING METHOD AND EQUIPMENT: Mobile B80 with 4-in solid stem augers (SPT tests were not conducted)  
 WATER LEVELS AND DATE: 18.0 ft 8/15/97 START: 8/14/97, 1300 FINISH: 8/14/97, 1400 LOGGER: R. Mokwa

DEPTH BELOW SURFACE (FT)	SAMPLE			STANDARD PENETRATION TEST RESULTS	SOIL DESCRIPTION	COMMENTS
	INTERVAL	NUMBER AND TYPE	RECOVERY (FT)			
0				6'-6'-6' (N)		
5					<u>SILTY SAND</u> , (SM), It brown, silt moist, fine-grained sand, silt plastic, some gravel to 1-in in size, mica particles evident.	This boring was conducted to probe for rock depth. SPT tests and sampling were not conducted. The soil descriptions given are based on the auger cutting returns as observed at the hole collar.
10					<u>SANDY SILT</u> , (ML), brown, moist, silt. plastic, some mica particles in cuttings.	
15					<u>SANDY SILT</u> , (ML), brown, moist, silt. plastic, clay balls in cuttings.	Driller reports formation becoming stiffer with depth.
20					<u>SANDY SILT</u> , (ML), brown, moist, silt. plastic.	Driller reports a gravel or cobble layer at 16.5 ft.
25					<u>SILT</u> , (ML), blue-gray, moist, plastic.	Smooth augering.
30					Auger refusal at 30.3 ft.	Driller reports gravel or cobble layer at 28 ft. Smooth augering from 28.5 to 30 ft. Auger refusal at 30.3 ft. Driller suspects very stiff layer, but reports drilling action does not indicate rock. Bottom of hole at 30.3 ft.

Figure C.1. Soil Boring Log BH-1.



The Charles Edward Via, Jr. Department of Civil Engineering	<b>BORING NUMBER</b> <b>BH-2</b>	<b>SHEET 1 OF 1</b>
<b>SOIL BORING LOG</b>		

PROJECT: Laterally Loaded Pile Cap Research LOCATION: Kentland Farms Site  
 ELEVATION: 98.80 ft DRILLING CONTRACTOR: Va Tech Geotechnical Department, Blacksburg, VA  
 DRILLING METHOD AND EQUIPMENT: Mobile B80 with 4-in solid stem augers and 140 lb drop hammer  
 WATER LEVELS AND DATE: none encountered START: 8/14/97, 1500 FINISH: 8/14/97, 1730 LOGGER: R. Mokwa

DEPTH BELOW SURFACE (FT)	SAMPLE			STANDARD PENETRATION TEST RESULTS	SOIL DESCRIPTION	COMMENTS
	INTERVAL	NUMBER AND TYPE	RECOVERY (FT)			
0						Topsoil 1.4 ft thick
2.5	2.5 - 4.0	SS-1	0.7	6-15-19 (34)	SANDY LEAN CLAY, CL, dk. brown, dry, hard, fine-grained, silt. organic, plastic.	Driller reports stiff layer at 4.0-4.3 ft 2-in broken rounded gravel piece in cuttings at 5 ft.
5.0	4.0 - 6.5	SS-2	1.5	6-10-14 (24)	SANDY LEAN CLAY, CL, brown, dry, very stiff, silt. plastic clay, fine-grained sand, mica particles evident.	
7.5	6.5 - 9.0	SS-3	1.5	5-6-10 (16)	SANDY SILT, ML, brown, silt. moist, very stiff, med. plastic silt, fine sand, some mica particles.	Smooth augering, little resistance to downthrust.
11.0	9.0 - 12.5	SS-4	1.5	3-5-6 (11)	SANDY SILT, ML, brown, silt. moist, stiff, med. plastic silt, fine sand, mica particles evident. (higher moisture content and more plastic than SS-3)	
15.5	12.5 - 17.0	SS-5	1.1	2-1-5 (6)	CLAYEY SAND, SC, gray, moist, loose, low plastic clay, fine sand, gravel pieces in end of spoon, 3-in layer of red-brown plastic clayey sand in center of sample.	Spoon bouncing on gravel piece during last 2 blows for SS-5. Driller reports gravelly layer at 17.5 - 18 ft.
20.5	17.0 - 20.9	SS-6	0.4	(50/4")	SILT, (ML), blue-gray, dry, hard, cemented, low plasticity, (pulverized weathered shale).	Bottom of hole @ 20.9 ft. Dry, stiff blue-gray silt on end of auger flights at 19 to bottom of hole.

Figure C.2. Soil Boring Log BH-2.



The Charles Edward Via, Jr. Department of Civil Engineering	BORING NUMBER <b>BH-3</b>	SHEET 1 OF 1
<b>SOIL BORING LOG</b>		

PROJECT: Laterally Loaded Pile Cap Research LOCATION: Kentland Farms Site  
 ELEVATION: 99.01 ft DRILLING CONTRACTOR: Va Tech Geotechnical Department, Blacksburg, VA  
 DRILLING METHOD AND EQUIPMENT: Mobile B80 with 4-in solid stem augers and 140 lb drop hammer  
 WATER LEVELS AND DATE: 18.2 ft 8/15/97 START: 8/15/97, 1000 FINISH: 8/15/97, 1300 LOGGER: R. Mokwa

DEPTH BELOW SURFACE (FT)	SAMPLE			STANDARD PENETRATION TEST RESULTS  6'-6'-6' (N)	SOIL DESCRIPTION  SOIL NAME, USCS GROUP SYMBOL, COLOR, MOISTURE CONTENT, RELATIVE DENSITY OR CONSISTENCY, SOIL STRUCTURE MINERALOGY	COMMENTS  DEPTH OF CASING, DRILLING RATE, DRILLING FLUID LOSS, TESTS AND INSTRUMENTATION
	INTERVAL	NUMBER AND TYPE	RECOVERY (FT)			
0						Topsoil 1.2 ft thick
2.5	2.5 - 4.0	SS-1	1.0	9-13-16 (29)	SANDY LEAN CLAY, CL, lt. brown, moist, very stiff, fine-grained sand, low plast. clay, mica particles evident.	
5	5.5 - 7.5	SS-2	1.4	7-10-15 (25)	SANDY SILT, ML, lt. brown, moist, very stiff, low plastic silt, fine sand, occnl. small 1/4" gravel, mica particles evident.	Driller reports augering thru a gravelly/cobbley layer from 5 to 5.5 ft. Smooth augering below 5.5 ft.
7.5	7.5 - 9.0	SS-3	1.5	5-8-10 (18)	SANDY SILT, ML, brown, moist, very stiff, low plastic silt, fine sand, occnl. small 3/4" gravel, some mica particles evident.	Smooth augering, little resistance to downthrust.
10	10.5 - 12.0	SS-4	1.5	5-4-6 (10)	SANDY SILT, ML, brown, moist, stiff, low plastic silt, fine sand, occnl. small 3/4" gravel, some mica particles evident.	
15	15.5 - 17.0	SS-5	1.4	2-4-6 (10)	SANDY LEAN CLAY, CL, brown, moist, stiff, low plastic clay, fine sand, gravel pieces in end of spoon.	Driller reports augering thru occnl. thin gravel layers from 15 to 20 ft. No difficulty in penetrating with the augers. Blue-gray silt appears in cuttings at 17 ft.
20	20.5 - 20.8	SS-6	0.4	38-50/3" (50/3")	SILTY CLAY WITH SAND, CL-ML, blue-gray, moist, hard, low plasticity, (pulverized weathered shale).	Bottom of hole @ 20.75 ft.

Figure C.3. Soil Boring Log BH-3.



The Charles Edward Via, Jr. Department of Civil Engineering	<b>BORING NUMBER</b> <b>BH-4</b>	SHEET 1 OF 1
<b>SOIL BORING LOG</b>		

PROJECT: Laterally Loaded Pile Cap Research

LOCATION: Kentland Farms Site

ELEVATION: 97.44 ft

DRILLING CONTRACTOR: Va Tech Geotechnical Department, Blacksburg, VA

DRILLING METHOD AND EQUIPMENT: Mobile B80 with 4-in solid stem augers and 140 lb drop hammer

WATER LEVELS AND DATE: 16.0, 1/26/98

START: 1/26/98, 13:30 FINISH: 1/26/98, 1640

LOGGER: R. Mokwa

DEPTH BELOW SURFACE (FT)	SAMPLE			STANDARD PENETRATION TEST RESULTS	SOIL DESCRIPTION	COMMENTS
	INTERVAL	NUMBER AND TYPE	RECOVERY (FT)	6'-6'-6" (N)	SOIL NAME, USCS GROUP SYMBOL, COLOR, MOISTURE CONTENT, RELATIVE DENSITY OR CONSISTENCY, SOIL STRUCTURE MINERALOGY	DEPTH OF CASING, DRILLING RATE, DRILLING FLUID LOSS, TESTS AND INSTRUMENTATION
0						
2.0	2.0 - 3.5	SS-1	1.2	5/9/17 (26)	<u>SANDY LEAN CLAY</u> , CL, dk. brown, moist, v. stiff, fine-grained, silt. organic, low plastic.	Driller reports gravelly layer from 2.5 to 3.5 ft. Encounter cobbles at 3.5'. Unable to penetrate with augers. Move rig 2' east and resume augering.
5	3.5 - 5.5					Smooth augering 3.5-5.0 ft.
5.5	5.5 - 6.4	ST-2	1.8	pushed 0.9'	<u>SANDY SILT</u> , (ML), brown, moist, low plast. silt, fine-grained sand.	Shelby tube ST-2 contains 0.9 ft of slough. Unable to advance ST-2 beyond 6.4' depth because of cobble or boulder.
6.4	6.4 - 7.5					Driller reports gravel layer from 6.4-7.0 ft. Smooth augering from 7-7.5 ft.
7.5	7.5 - 9.8	ST-3	2.3	pushed 2.3' med. resistance	<u>SANDY LEAN CLAY</u> , CL, dk. brown, moist, fine-grained sand, low plastic silt.	Smooth augering, little resistance to downthrust. Obtain bag sample of auger cuttings at 10-11.0 ft.
9.8	9.8 - 11.3	SS-4	1.5	7-11-14 (25)	<u>SANDY LEAN CLAY</u> , CL, dk. brown, moist, v. stiff, fine-grained sand, low plastic silt.	
11.3	11.3 - 12.0	ST-5	2.3	pushed 2.3' (easy push)		
12.0	12.0 - 14.3	SS-6	0.1	4-1-1 (2) cuttings	<u>POORLY GRADED SILTY SAND</u> (SP), brown, wet, v. loose, low plasticity.	Smooth augering.
14.3	14.3 - 15.8				<u>SANDY LEAN CLAY</u> , CL, dk. brown, moist, v. stiff, fine-grained sand, low plastic silt.	Measured GWT at 16.0 ft after SS-6. Obtain bag sample of auger cuttings at 16-16.5 ft.
15.8	15.8 - 16.5	SS-7	0.1	10-50/1" (50/1")	<u>SILT</u> , ML, brown-gray, wet, low plasticity, v. hard.	Driller reports difficult advancement at 16 ft.
16.5	16.5 - 17.1					Bottom of hole @ 17.1 ft.
17.1						

Figure C.4. Soil Boring Log BH-4.



The Charles Edward Via, Jr. Department of Civil Engineering	<b>BORING NUMBER</b> <b>BH-5</b>	<b>SHEET 1 OF 1</b>
<b>SOIL BORING LOG</b>		

PROJECT: Laterally Loaded Pile Cap Research LOCATION: Kentland Farms Site  
 ELEVATION: 97.72 ft DRILLING CONTRACTOR: Va Tech Geotechnical Department, Blacksburg, VA  
 DRILLING METHOD AND EQUIPMENT: Mobile B80 with 4-in solid stem augers and 140 lb drop hammer  
 WATER LEVELS AND DATE: 15.4, 1/25/98 START: 2/2/98, 12:15 FINISH: 2/2/98, 15:15 LOGGER: R. Mokwa

DEPTH BELOW SURFACE (FT)	SAMPLE			STANDARD PENETRATION TEST RESULTS 6'-6" (N)	SOIL DESCRIPTION	COMMENTS
	INTERVAL	NUMBER AND TYPE	RECOVERY (FT)			
	0	0.0	ST-1			
	2.1					
	3.6					
5	5.9	ST-2	2.3	pushed 2.3'		
	8.2	ST-3	2.3	pushed 2.3'		
	10.5	ST-4	2.3	pushed 2.3'		
	12.8	ST-5	2.3	pushed 2.3'		
15	15.1	ST-6	2.3	pushed 2.3'		
				auger cuttings		
20						
25						

Figure C.5. Soil Boring Log BH-5.



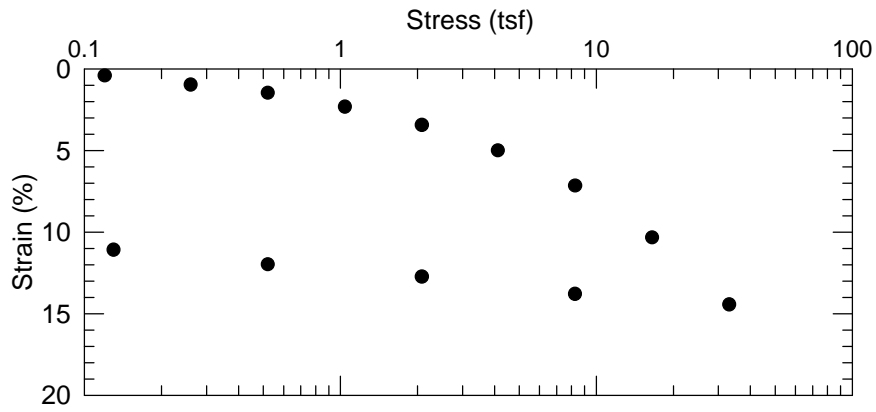
The Charles Edward Via, Jr. Department of Civil Engineering	BORING NUMBER <b>BH-6</b>	SHEET 1 OF 1
<b>SOIL BORING LOG</b>		

PROJECT: Laterally Loaded Pile Cap Research LOCATION: Kentland Farms Site  
 ELEVATION: 98.04 ft DRILLING CONTRACTOR: Va Tech Geotechnical Department, Blacksburg, VA  
 DRILLING METHOD AND EQUIPMENT: Mobile B50 with 4-in solid stem augers and 140 lb drop hammer  
 WATER LEVELS AND DATE: None Encountered START: 1/26/98, 15:00 FINISH: 1/26/98, 15:40 LOGGER: R. Mokwa

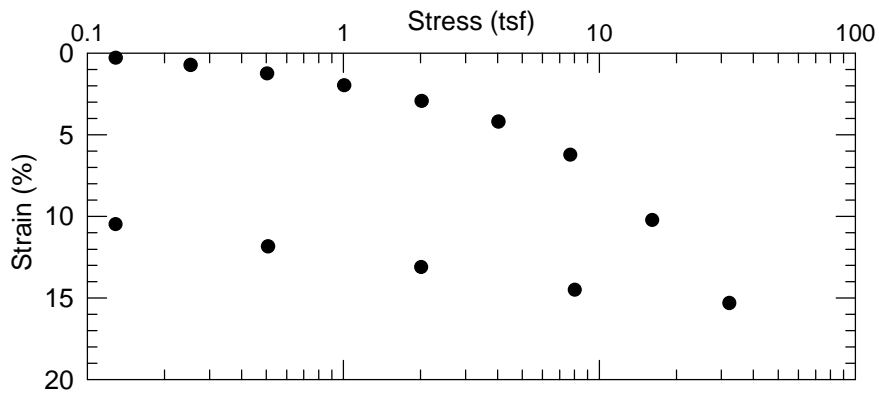
DEPTH BELOW SURFACE (FT)	SAMPLE			STANDARD PENETRATION TEST RESULTS  6'-6" (2)	SOIL DESCRIPTION  SOIL NAME, USCS GROUP SYMBOL, COLOR, MOISTURE CONTENT, RELATIVE DENSITY OR CONSISTENCY, SOIL STRUCTURE MINERALOGY	COMMENTS  DEPTH OF CASING, DRILLING RATE, DRILLING FLUID LOSS, TESTS AND INSTRUMENTATION
	INTERVAL	NUMBER AND TYPE	RECOVERY (FT)			
0	0.5	SS-1	1.5	3-4-7 (11)	SANDY LEAN CLAY, CL, dk. brown, moist, stiff, fine-grained, silt. organic, low plastic.	Very difficult to push ST-2. Shelby tube bent during push and the bottom was partially crushed. Considerable sample disturbance likely.  Bottom of hole @ 5.8 ft.
	2.0					
5	3.5	ST-2	1	pushed 2.3	SANDY LEAN CLAY, CL, dk. brown, moist, soft, fine-grained, silt. organic, low plastic.	
	5.8					

Figure C.6. Soil Boring Log BH-6.

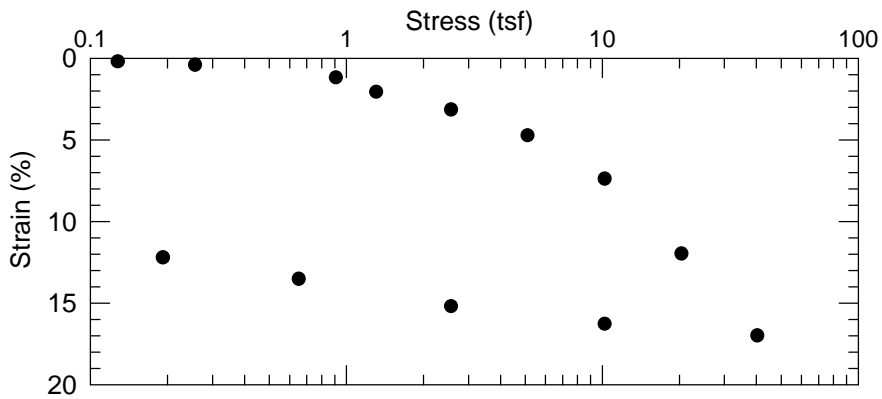
**APPENDIX D**  
**LABORATORY TEST RESULTS**



(a) Sample BH5-ST-3



(b) Sample BH5-ST-4



(c) Sample BH4-ST-5

Figure D.1. Consolidation curves for natural soil, strain vs. log p.

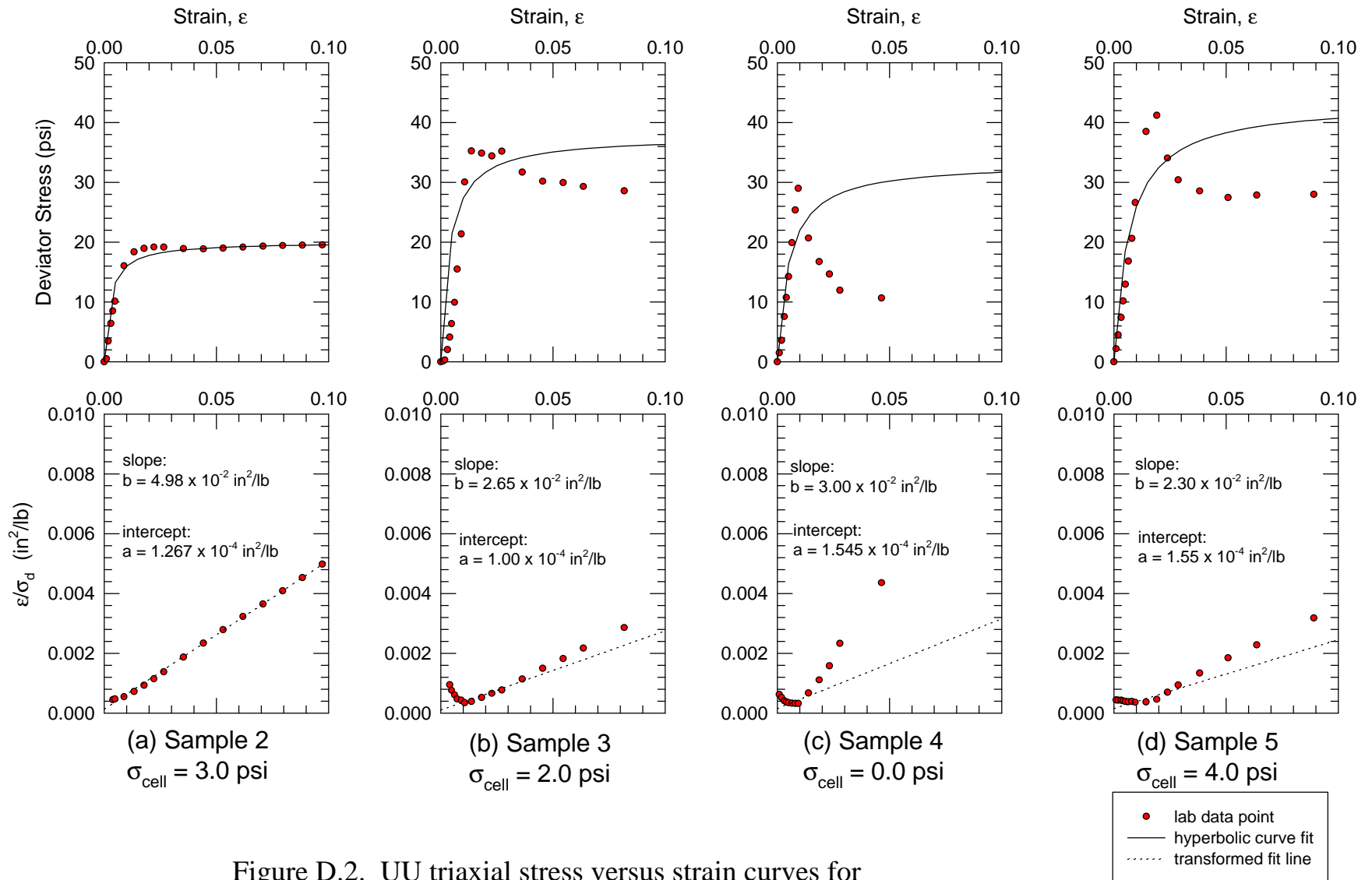


Figure D.2. UU triaxial stress versus strain curves for natural soil (1 of 3).

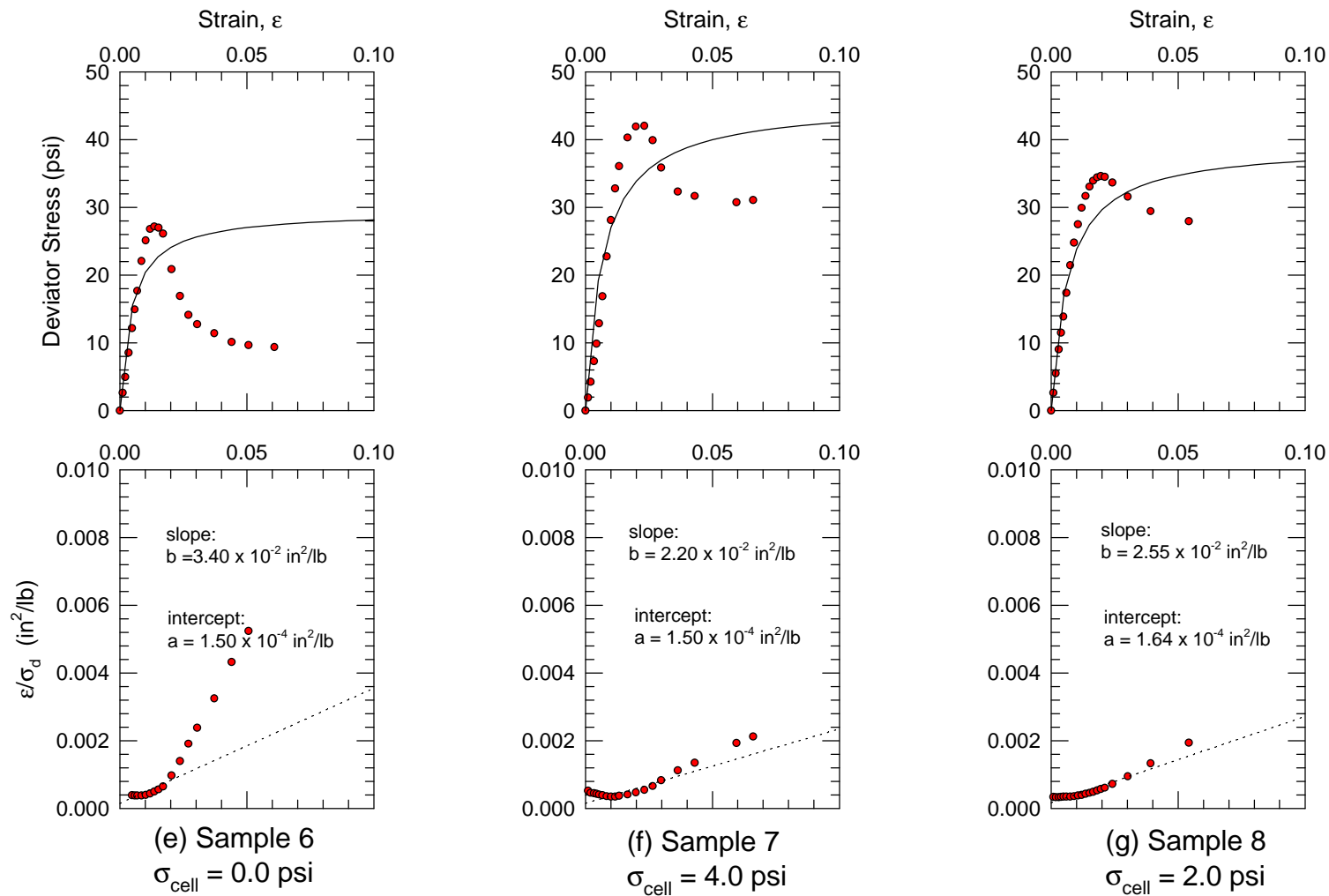


Figure D.3. UU triaxial stress versus strain curves for natural soil (2 of 3).

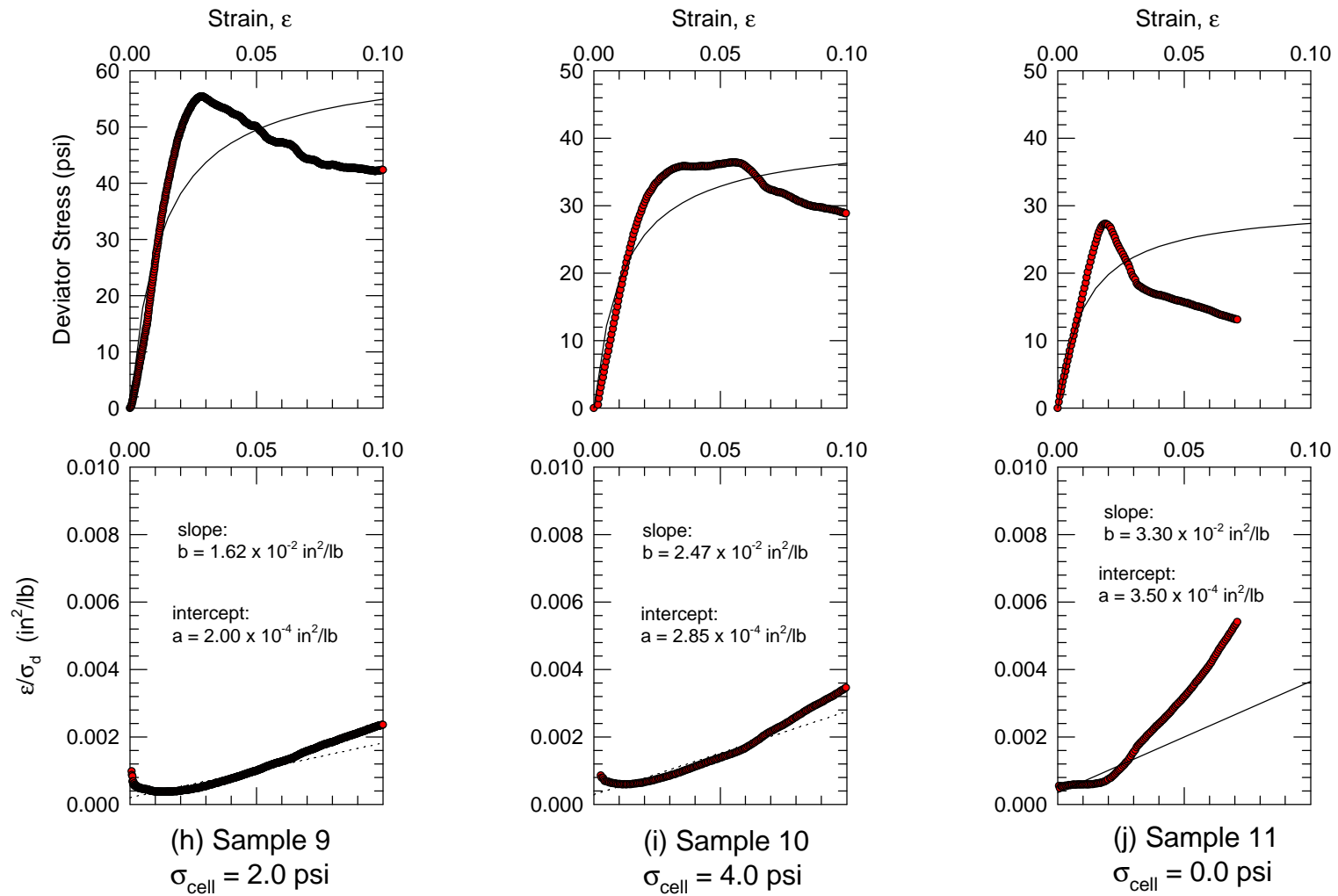


Figure D.4. UU triaxial stress versus strain curves for natural soil (3 of 3).

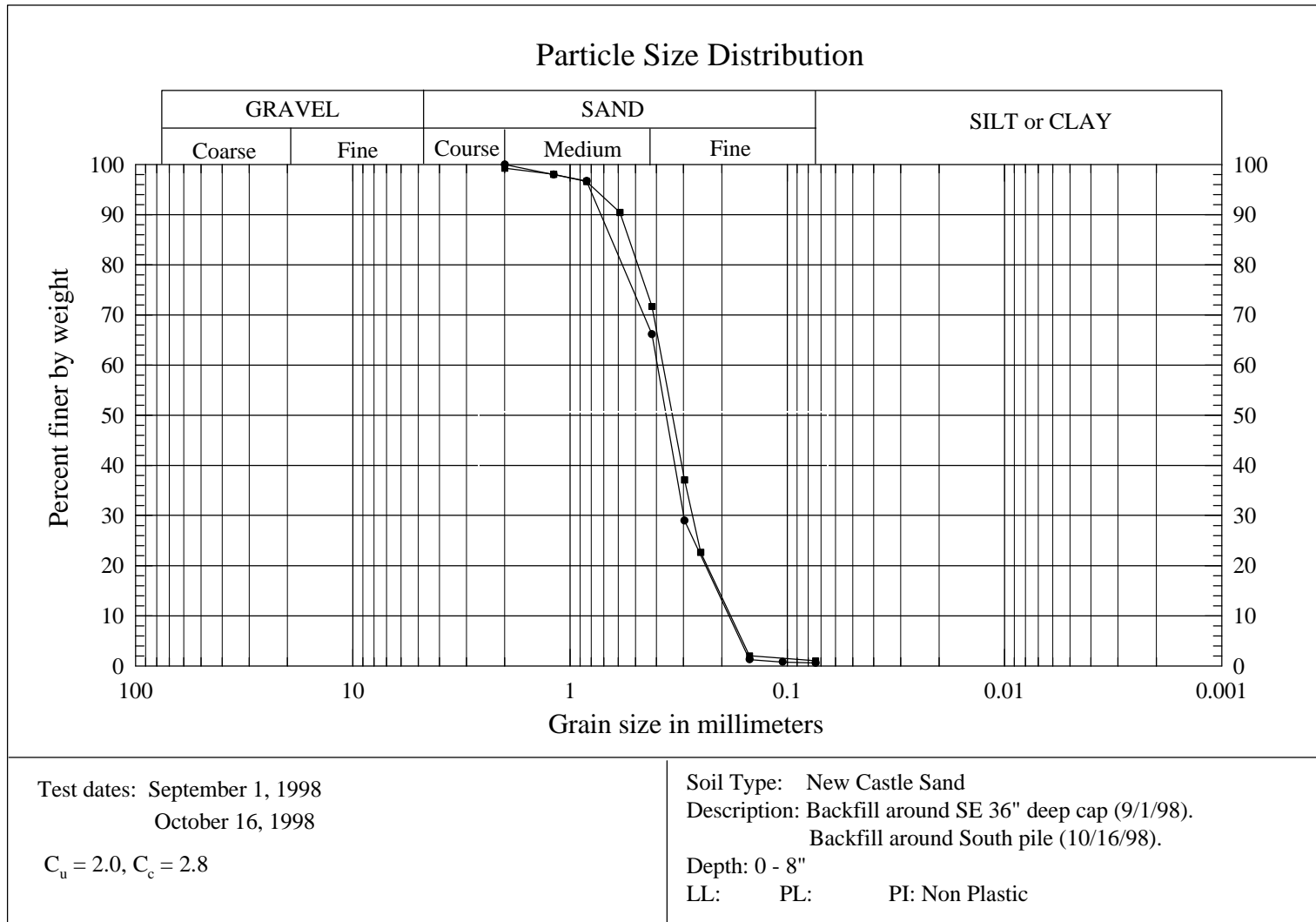


Figure D.5. Grain size distribution curves for New Castle Sand.

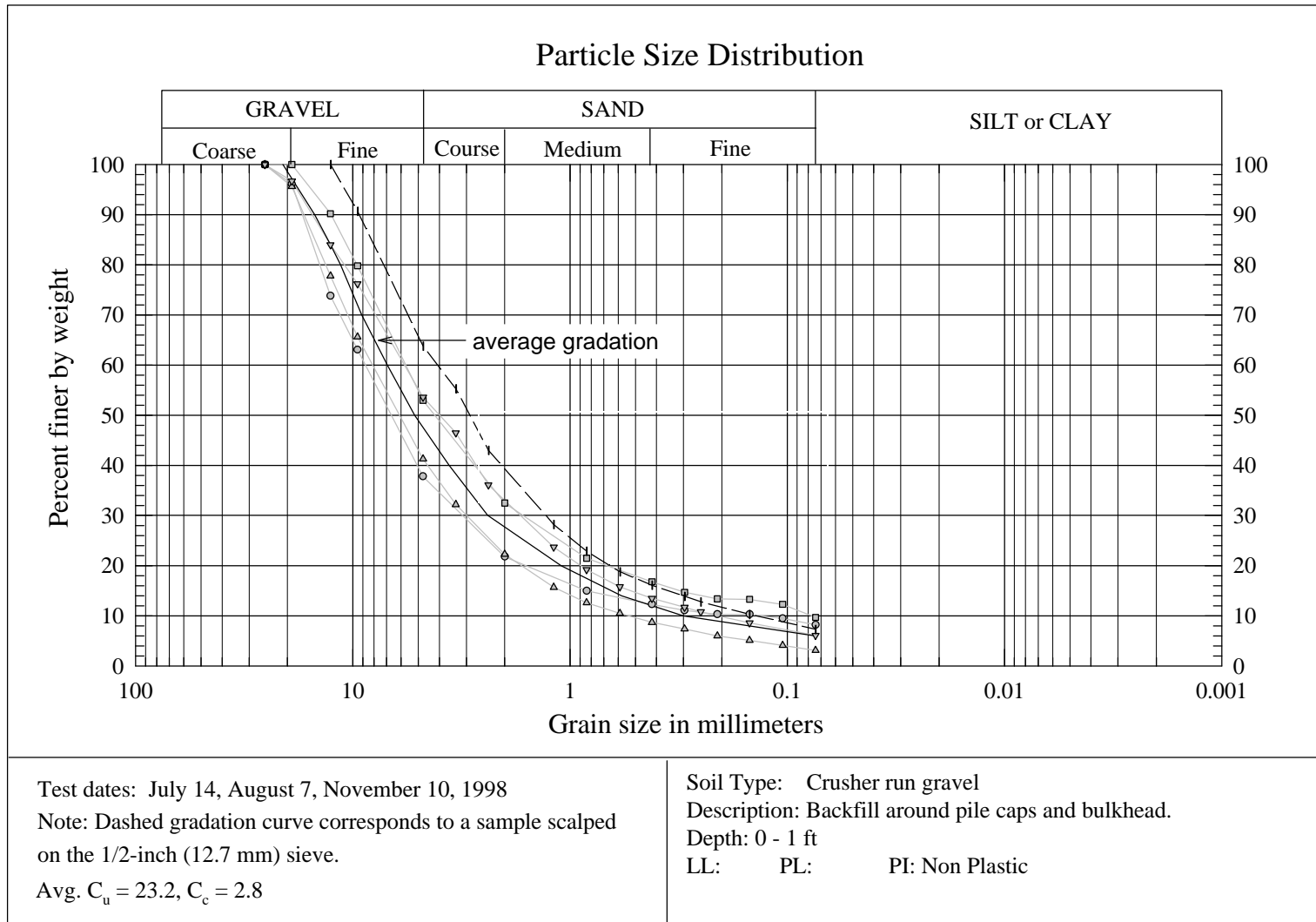
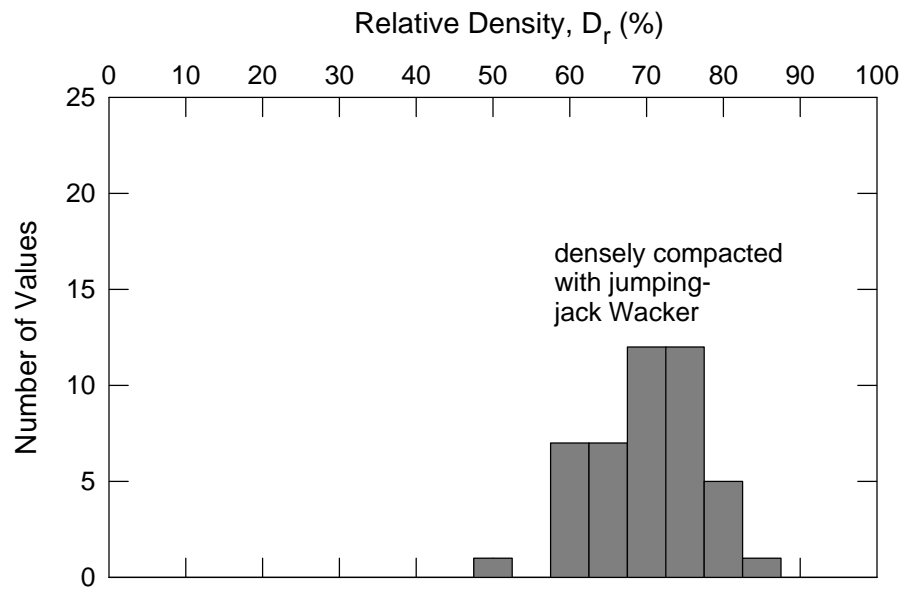
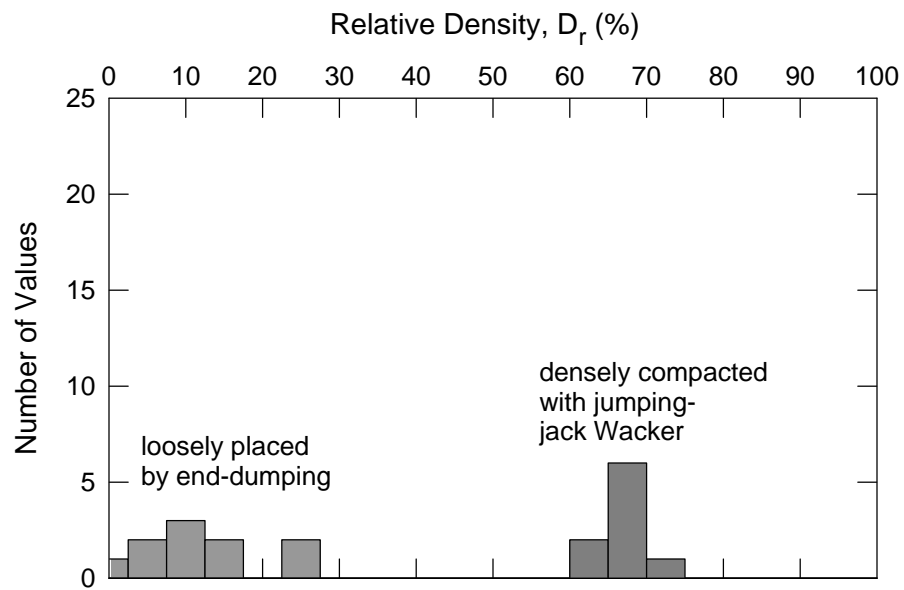


Figure D.6. Grain size distribution curves for crusher run gravel.



(a) Crusher run gravel.



(b) New Castle sand.

Figure D.7. Distribution of relative density values based on nuclear gage field test results.

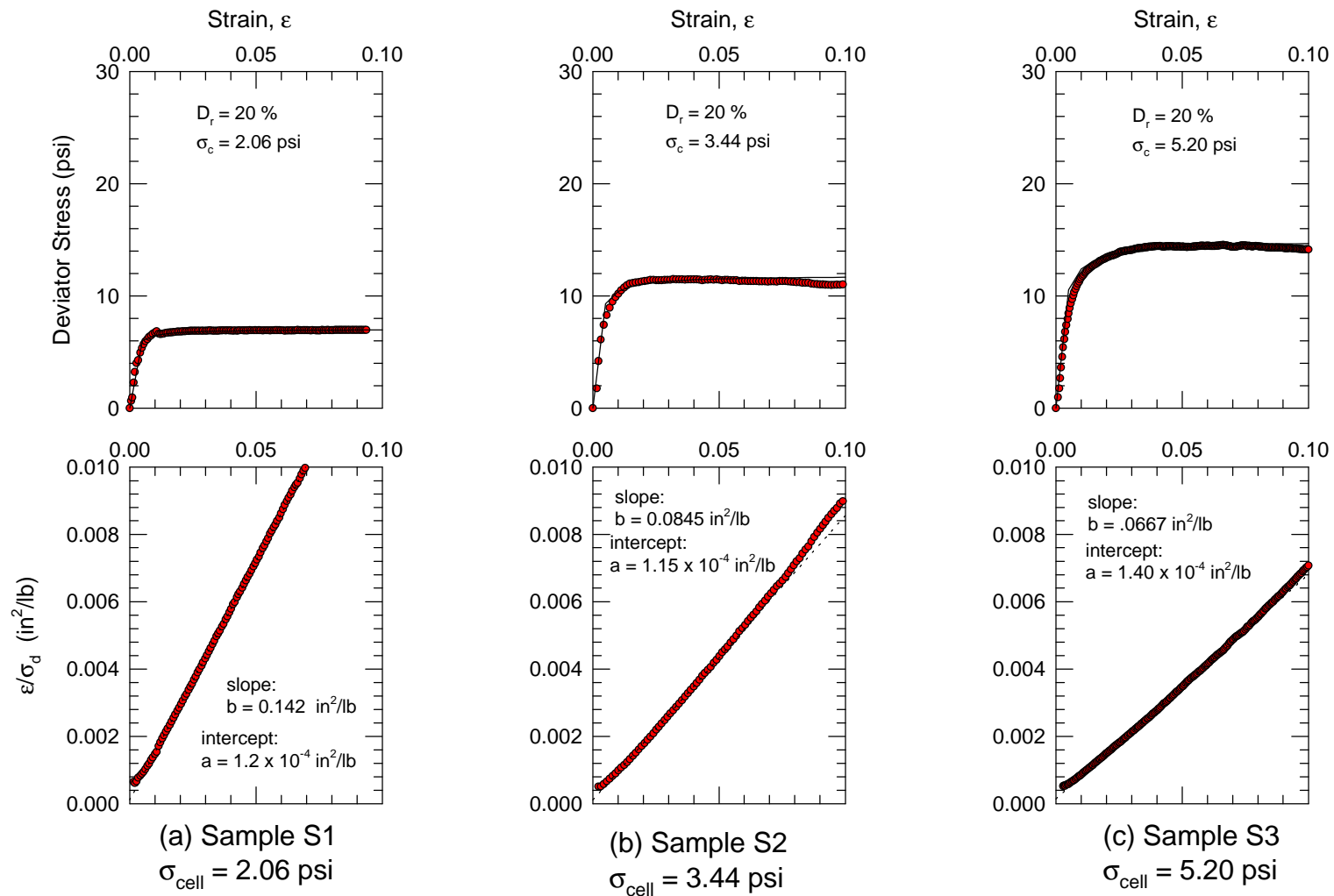


Figure D.8. CD triaxial stress versus strain curves for New Castle sand,  $D_r = 20\%$ , (1 of 3).

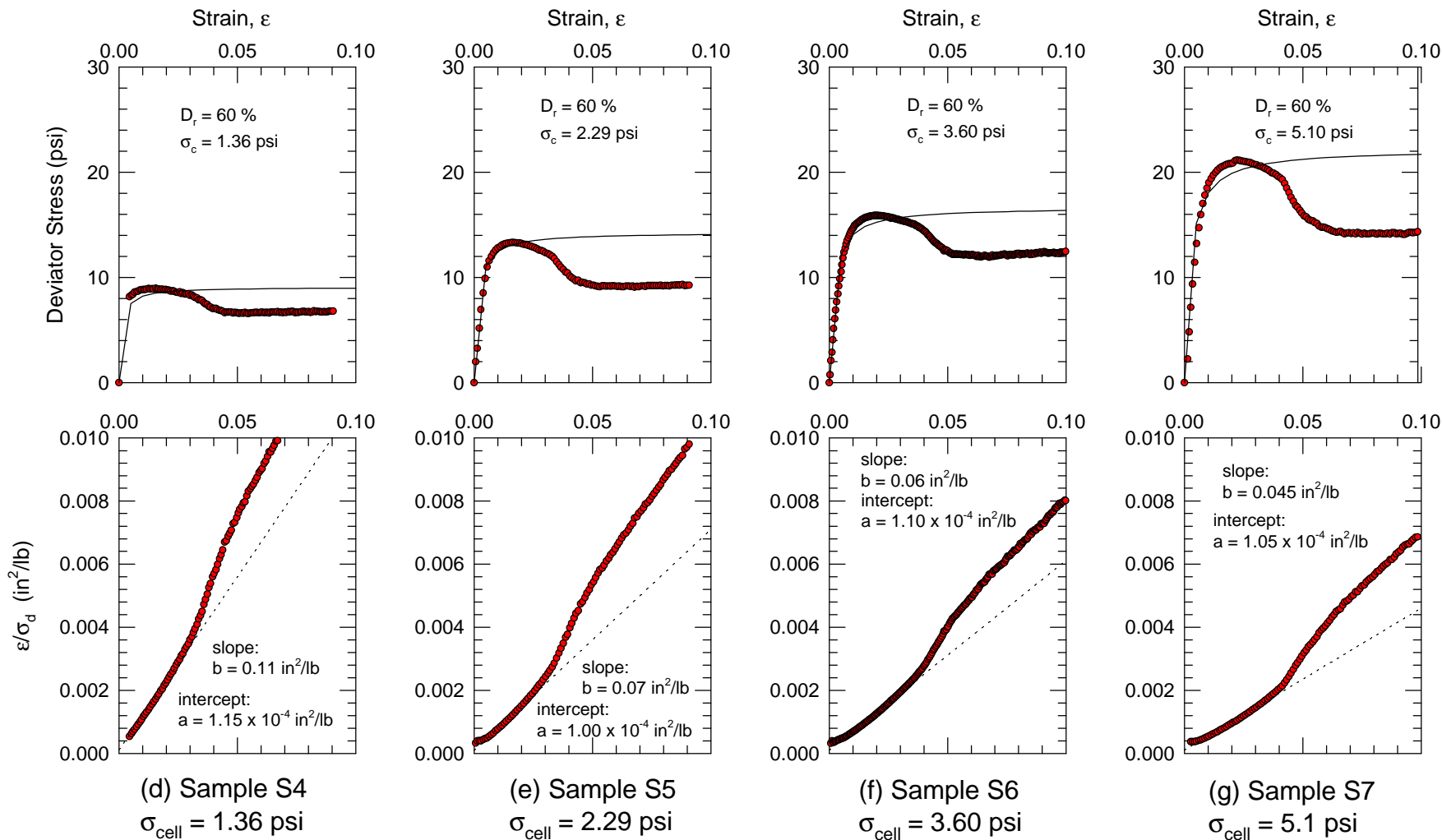


Figure D.9. CD triaxial stress versus strain curves for New Castle sand,  $D_r = 60\%$ , (2 of 3).

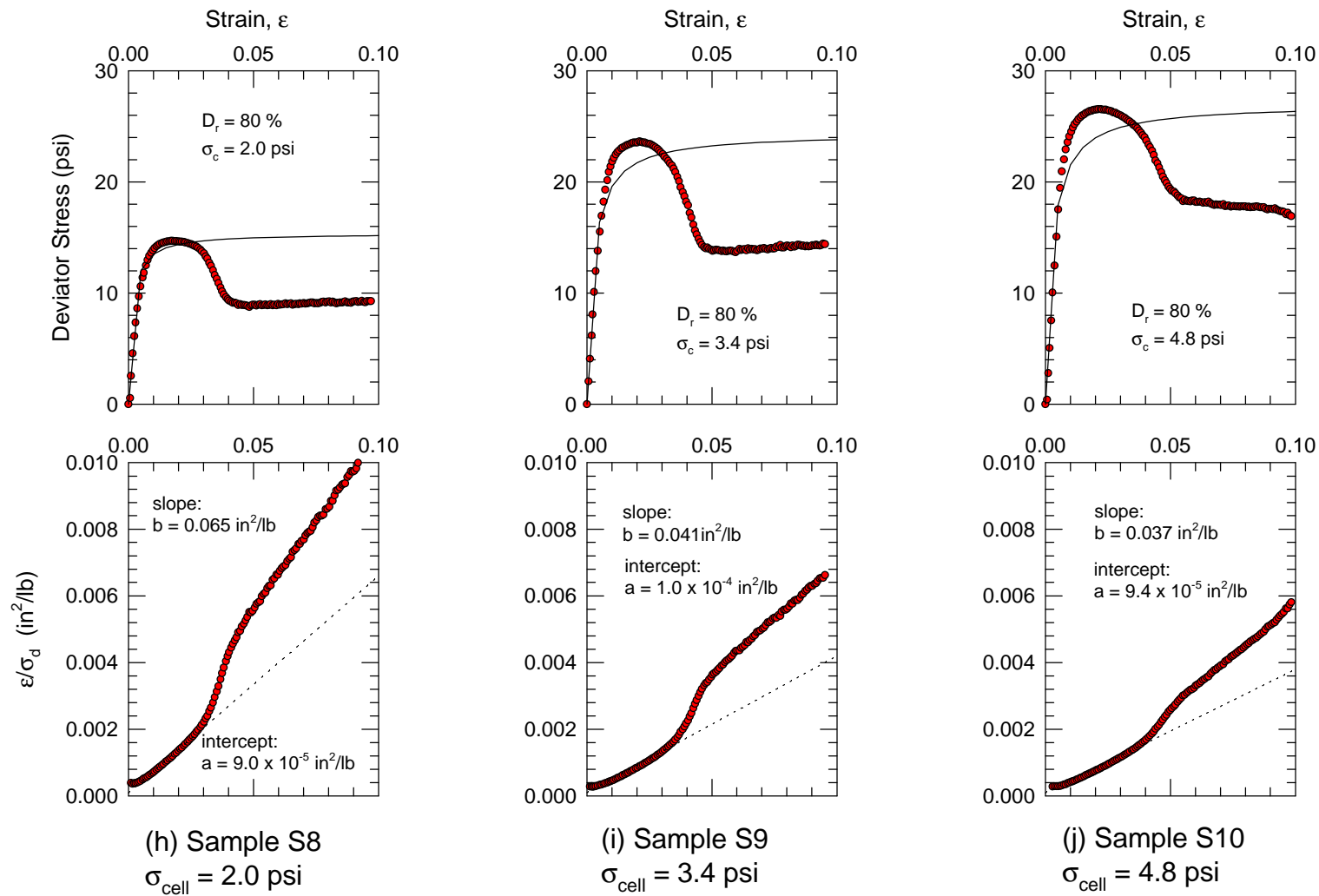


Figure D.10. CD triaxial stress versus strain curves for New Castle sand,  $D_r = 80\%$ , (3 of 3).

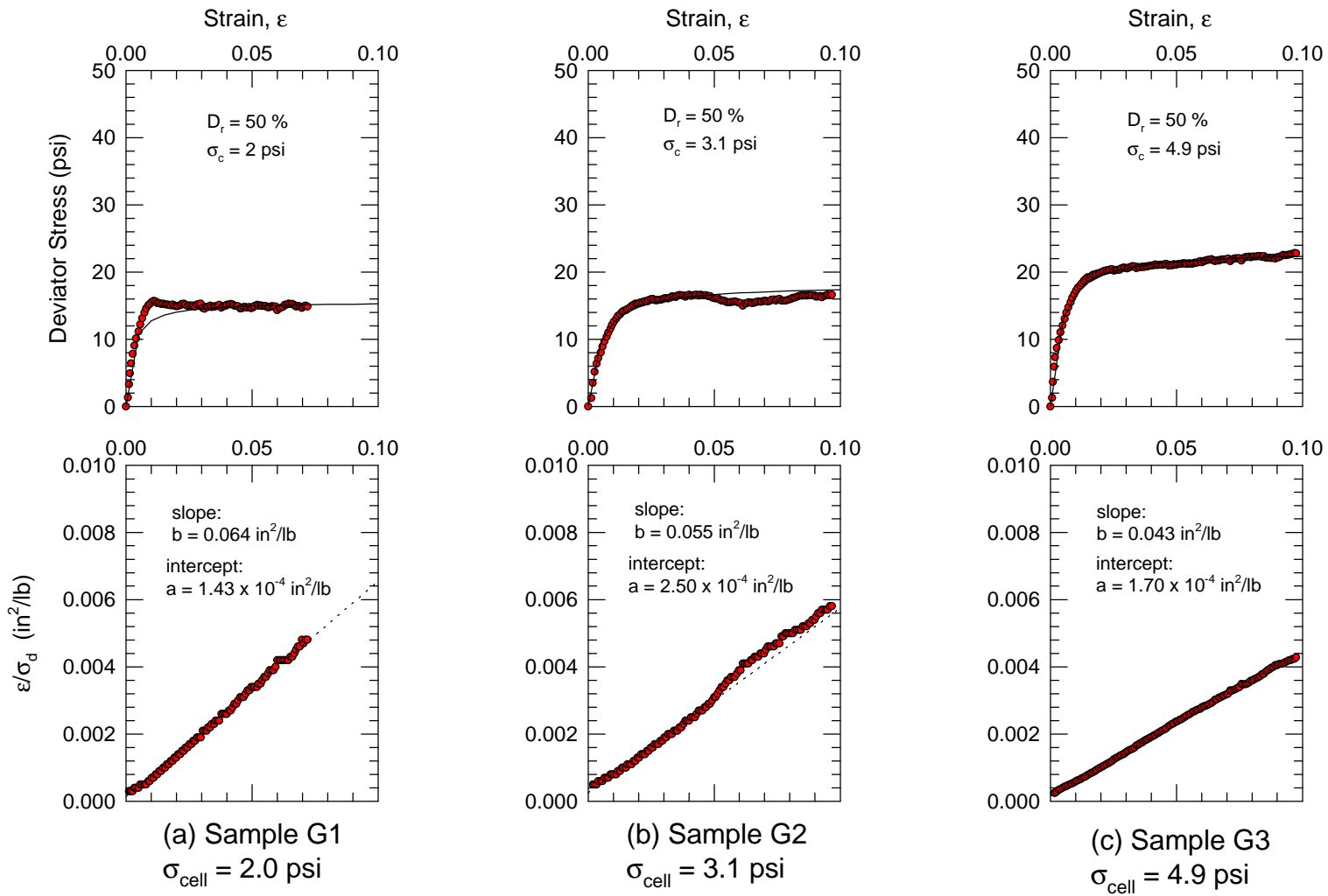


Figure D.11. CD triaxial stress versus strain curves for crusher run gravel,  $D_r = 50\%$ , (1 of 3).

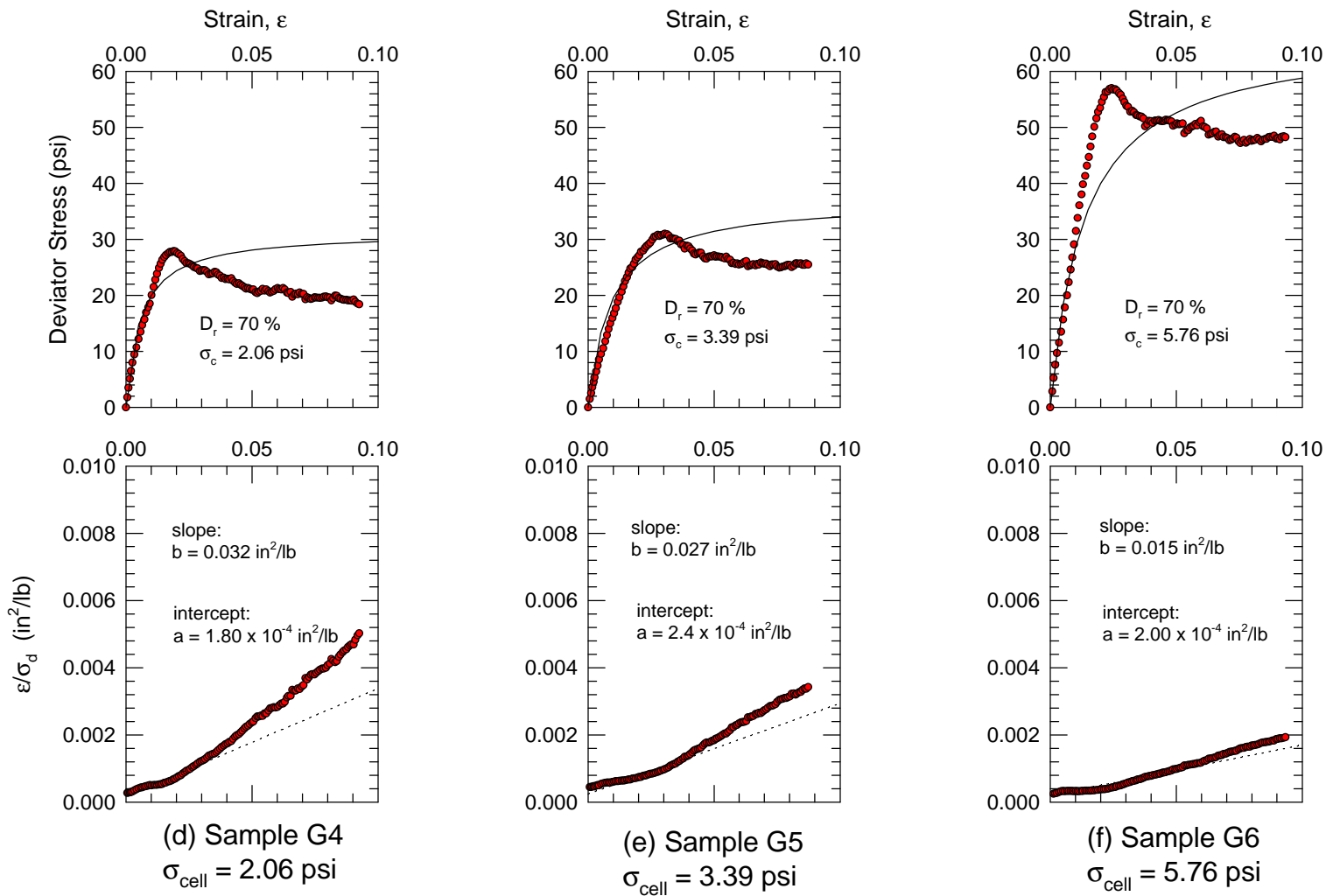
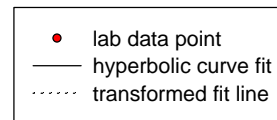


Figure D.12. CD triaxial stress vs. strain curves for recompacted samples of crusher run gravel,  $D_r = 70\%$ , (2 of 3).



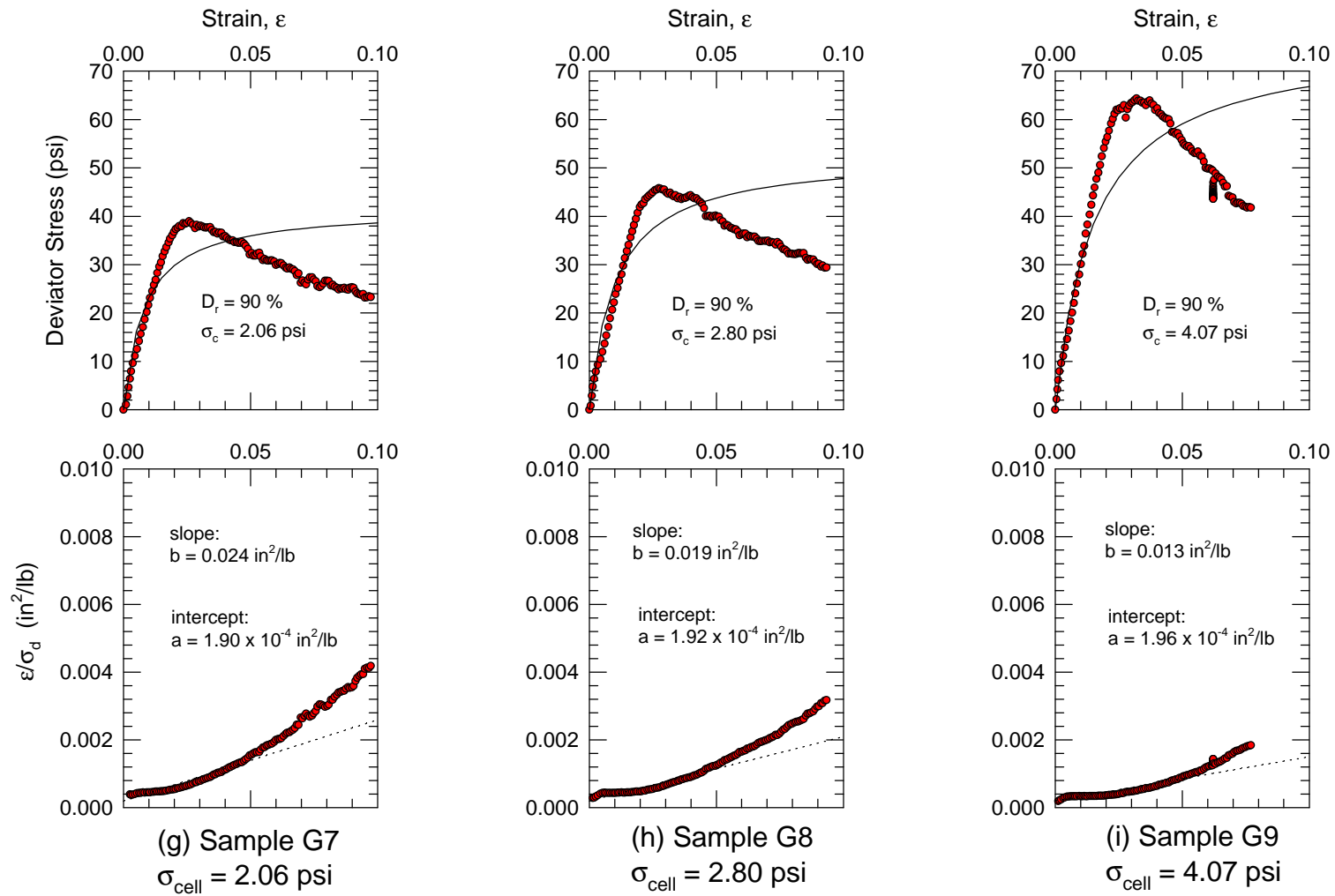


Figure D.13. CD triaxial stress vs. strain curves for recomacted samples of crusher run gravel,  $D_r = 90\%$ , (3 of 3).

## APPENDIX E - EQUATIONS FOR $K_q$ AND $K_c$ FACTORS FOR THE BRINCH-HANSEN (1961) THEORY

### E.1 Introduction

Included in this Appendix are the equations used to calculate the earth pressure coefficients for Brinch-Hansen's (1961) theory. These coefficients account for three-dimensional loading effects of soils that possess both cohesion and friction.

### E.2 Equations for $K_q$ and $K_c$

$$K_q = \frac{K_q^o + K_q^\infty a_q \frac{x}{D}}{1 + a_q \frac{x}{D}} \quad \text{Equation E.1}$$

where:

$K_q$  = passive earth pressure coefficient due to weight of soil at intermediate depth,

$K_q^o$  = passive earth pressure coefficient due to weight of soil at ground surface,

$$K_q^o = \left( e^{\left(\frac{1}{2}\pi + \phi\right)\tan\phi} \cos\phi \tan\left(45^\circ + \frac{1}{2}\phi\right) - \left( e^{-\left(\frac{1}{2}\pi - \phi\right)\tan\phi} \cos\phi \tan\left(45^\circ - \frac{1}{2}\phi\right) \right) \right)$$

$K_q^\infty$  = passive earth pressure coefficient due to weight of soil at great depth,

$$K_q^\infty = N_c d_c^\infty K_o \tan\phi,$$

$$\alpha_q = \frac{K_q^o K_o \sin\phi}{(K_q^\infty - K_q^o) \sin\left(45^\circ + \frac{1}{2}\phi\right)}$$

$x$  = depth below ground (units of length),

$D$  = shaft diameter (units of length),

$K_o$  = at-rest earth pressure,

$K_o = 1 - \sin\phi$ , and

$\phi$  = friction angle of foundation soil.

$$K_c = \frac{K_c^o + K_c^\infty a_c \frac{x}{D}}{1 + a_c \frac{x}{D}} \quad \text{Equation E.2}$$

where:

$K_c$  = passive earth pressure coefficient due to cohesion at intermediate depth,

$K_c^o$  = passive earth pressure coefficient due to cohesion at ground surface,

$$K_c^o = [e^{(\frac{1}{2}\pi + \phi)\tan\phi} \cos\phi \tan(45^\circ + \frac{1}{2}\phi) - 1] \cot\phi,$$

$K_c^\infty$  = passive earth pressure coefficient due to cohesion at great depth,

$$K_c^\infty = N_c d_c^\infty$$

$$\alpha_c = \frac{K_c^o}{K_c^\infty - K_c^o} 2 \sin(45^\circ + \frac{1}{2}\phi),$$

$\phi$  = friction angle of foundation soil,

$N_c$  = bearing capacity factor,

$$N_c = [e^{\pi \tan\phi} \tan^2(45^\circ + \frac{1}{2}\phi) - 1] \cot\phi,$$

$d_c^\infty$  = depth coefficient at great depth, and

$$d_c^\infty = 1.58 + 4.09 \tan^4 \phi.$$

## APPENDIX F – LOG SPIRAL EARTH PRESSURE THEORY

### F.1 Introduction

This Appendix describes the approach used to calculate passive earth pressures using the log spiral theory. Dr. J. M. Duncan developed an early version of this numerical analysis procedure. The equations presented in this appendix were coded in an *EXCEL* macro using the Visual Basic Applications programming language. The macro program is embedded in an *EXCEL* workbook named *PYCAP*, which was developed by the author for calculating p-y curves for embedded pile caps. The workbook *PYCAP* contains a number of different worksheets. Log spiral earth pressure calculations are performed in the worksheet named *Log Spiral*. Although the procedure described in this appendix was initially developed for pile caps, it applies equally as well to retaining walls, bulkheads, and other backfilled or embedded structures.

In the passive zone, the theoretical failure surface consists of two zones: 1) the Prandtl zone, which is bounded by a logarithmic spiral, and 2) the Rankine zone, which is bounded by a plane, as shown in Figure F.1(a). The shape of the log spiral failure surface, is shown in Figure F.1(b). The theory is based on the principle that force vectors acting on the log spiral failure surface make angles of  $\phi$  with the tangent to the spiral, and the lines of action of the force vectors pass through the center of the spiral.

The procedure described in this appendix was used to determine the ultimate passive earth pressure,  $E_p$ , and the individual components of  $E_p$ , which can be described as:

$$E_p = (P_{p\phi} + P_{pc} + P_{pq}) \quad \text{Equation F.1}$$

where  $E_p$  is the ultimate passive earth pressure force per unit length (force/length),  $P_{p\phi}$  is the component due to soil weight and friction (force/length),  $P_{pc}$  is the component due to soil cohesion (force/length),  $P_{pq}$  is the component due to surcharge (force/length), and  $b$  is the cap width or the length of the wall. Performing the calculations in this manner provides a means of isolating the three primary components of passive earth pressure. The contribution from

each component is computed using the log spiral earth pressure theory, as described in the following sections.

## F.2 Log Spiral Numerical Approximation

The procedure used to determine the components of  $E_p$  is described in this section. The procedure uses the trigonometric properties of the log spiral, as shown in Figure F.1(b). The equation defining the log spiral surface is:

$$r = r_o e^{(q \tan \phi \theta)} \quad \text{Equation F.2}$$

where  $r$  is the radius of the log spiral at an angle  $\theta$  from  $r_o$ ,  $r_o$  is the starting radius that positions the spiral onto the wall-soil geometry,  $\theta$  is the angle between  $r$  and  $r_o$ , and  $\phi$  is the soil friction angle. This equation forms the kernel of the iterative technique, which is based on equations of equilibrium and geometry. The primary variables and dimensions used in the procedure are shown in Figure F.2.

The minimum value of passive earth pressure is determined by iteration. An initial value of the dimension  $w$  is assumed, and the corresponding value of the passive earth pressure force ( $E_p$ ) is computed as described in the following pages. The value of  $E_p$  includes all three components:  $P_{p\phi}$ ,  $P_{pc}$ , and  $P_{pq}$ . The iteration loop is repeated by assuming a smaller or larger value of  $w$  and another value of the passive earth pressure force is computed. If this value of  $E_p$  is smaller than the first computed value of  $E_p$ , the value of  $w$  is adjusted again. By adjusting the assumed value of  $w$  (larger or smaller), the minimum value of  $E_p$  is computed with an accuracy of 0.005 %.

The program determines the location of the center of the log spiral by iterating on the values of  $r$  and  $x_o$  until the dimensions of the failure surface are consistent. After determining the geometry and sizes of the failure zones, the earth pressure forces are determined from equilibrium, assuming the shear strength of the soil is fully mobilized along the slip surface.

The procedure is started by determining the shape of the failure surface, using the following equations:

$$\mathbf{a} = 45 - \frac{\mathbf{f}}{2} \quad \text{Equation F.3.a}$$

$$w = \overline{af} \quad \text{Equation F.3.b}$$

$$H_d = \overline{df} = w \tan \mathbf{a} \quad \text{Equation F.3.c}$$

$$y_o = x_o \tan \mathbf{a} \quad \text{Equation F.3.d}$$

$$r_o = \sqrt{(H + y_o)^2 + x_o^2} \quad \text{Equation F.3.e}$$

$$\mathbf{q}_{\max} = 90 - \tan^{-1} \left( \frac{x_o}{H + y_o} \right) - \mathbf{a} \quad \text{Equation F.3.f}$$

$$r = \sqrt{w^2 + H_d^2} + \frac{x_o}{\sqrt{x_o^2 + y_o^2}} \sqrt{x_o^2 + y_o^2} \quad \text{Equation F.3.g}$$

The log spiral surface is fitted to the wall geometry and soil shear strength using the following steps:

1. Compute  $H_d$  using Equation F.3.c
2. Assume an initial value of  $x_o$
3. Compute  $y_o$  using Equation F.3.d
4. Compute  $r_o$  using Equation F.3.e
5. Compute  $\theta$  using Equation F.3.f
6. Compute  $r$  using the log spiral Equation, F.2
7. Compute  $r$  using Equation F.3.g
8. Compare the computed  $r$  values from steps 6 and 7

9. If the  $r$  values are in agreement with the tolerances established, continue with the procedure, otherwise, return to step 2 and modify  $x_o$

The following steps are used to estimate the weight of soil within the log spiral failure zone (defined by points abdf), and the location of the weight resultant,  $W$ , as shown in Figure F.3(a).

Compute the dimensions and centroid of area abdf, shown in Figure F.3.

$$H_d = r \sin \mathbf{a} - y_o \quad \text{Equation F.4.a}$$

$$l_1 = \frac{2}{3} H + y_o \quad \text{Equation F.4.b}$$

$$k = w \frac{H + 2H_d}{3(H + H_d)} \quad \text{Equation F.4.c}$$

$$l_2 = x_o + k \quad \text{Equation F.4.d}$$

$$l_3 = \frac{2}{3} H_d + y_o \quad \text{Equation F.4.e}$$

Calculate the soil weight,  $W$ , by estimating the area enclosed by points abdf:

$$W = \gamma [\text{Area within the log spiral from b to d } (A_{1s}) - \text{Area of triangle oab } (A_{t1}) + \text{Area of triangle adf } (A_{t2})]$$

$$W = \gamma [A_{1s} - A_{t1} + A_{t2}]$$

$$W = \mathbf{g} \left( \frac{r_1^2 - r_o^2}{4 \tan \mathbf{f}} - \frac{1}{2} x_o H + \frac{1}{2} w H_d \right) \quad \text{Equation F.5}$$

Break  $E_p$  into its horizontal and vertical components:

$$\text{horizontal component} = E_p \cos \delta$$

$$\text{vertical component} = E_p \sin \delta$$

Using equilibrium, determine  $P_{p\phi}$ ,  $P_{pc}$ , and  $P_{pq}$ , as described below.

**Compute  $P_{pf}$  - the earth pressure due to weight of soil.** (Refer to Figure F.3a.)

The soil above the top of the wall is treated as a surcharge, and its strength is ignored in the calculations. Calculate the Rankine earth pressure due to soil weight,  $E_{PRf}$ , acting on the vertical face defined by points  $df$ :

$$E_{PRf} = \frac{1}{2} g H_d^2 \tan^2 \left( 45 + \frac{f}{2} \right) \quad \text{Equation F.6}$$

Calculate  $P_{p\phi}$  by summing moments about the spiral origin, point O:

$$P_{pf} = \frac{l_2 W + l_3 E_{PRf}}{(l_1 \cos d - x_o \sin d)} \quad \text{Equation F.7}$$

**Compute  $P_{pc}$  - earth pressure due to cohesion.** (Refer to Figure F.3b.)

$$l_4 = x_o + \frac{w}{2} \quad \text{Equation F.8}$$

$$l_5 = y_o + \frac{H_d}{2} \quad \text{Equation F.9}$$

Calculate the Rankine earth pressure due to cohesion,  $E_{PRc}$ , acting on the vertical face defined by points  $df$ :

$$E_{PRc} = 2c \tan \left( 45 + \frac{f}{2} \right) H_d \quad \text{Equation F.10}$$

Calculate the moment due to cohesion,  $M_c$ , about point O:

$$M_c = \frac{c}{2 \tan \mathbf{f}} (r_1^2 - r_o^2) \quad \text{Equation F.11}$$

Calculate  $P_{pc}$  by summing moments about point O:

$$P_{pc} = \frac{M_c + l_5 E_{PRc} + \alpha c H x_o}{(l_1 \cos \mathbf{d} - x_o \sin \mathbf{d})} \quad \text{Equation F.12}$$

where  $\alpha$  is the adhesion between the cohesive soil and wall, the factor  $\alpha$  can range from 0 to 1.

**Compute  $P_{pq}$  - earth pressure due to surcharge.** (Refer to Figure F.3c.)

Calculate the Rankine earth pressure due to surcharge,  $E_{PRq}$ , acting on the vertical face defined by points df:

$$E_{PRq} = q_s \tan^2 \left( 45 + \frac{\mathbf{f}}{2} \right) H_d \quad \text{Equation F.13}$$

Calculate  $P_{pq}$  by summing moments about point O:

$$P_{pq} = \frac{l_4 w q_s + l_5 E_{PRq}}{(l_1 \cos \mathbf{d} - x_o \sin \mathbf{d})} \quad \text{Equation F.14}$$

### F.3 Log Spiral Solution

The individual components can be combined to compute the ultimate passive earth pressure,  $E_p$ , in units of force per unit length, as follows:

$$E_p = (P_{p\phi} + P_{pc} + P_{pq}) \quad \text{Equation F.15}$$

where  $P_{p\phi}$  is the component due to soil weight and friction,  $P_{pc}$  is the component due to soil cohesion,  $P_{pq}$  is the component due to surcharge, and  $b$  is the width of the cap or wall.

The earth pressure coefficient for friction and soil weight is defined as:

$$K_{pf} = \frac{2P_{pf}}{gH^2} \quad \text{Equation F.16a}$$

the earth pressure coefficient for cohesion is defined as:

$$K_{pc} = \frac{P_{pc}}{2cH} \quad \text{Equation F.16b}$$

and the earth pressure coefficient for surcharge is defined as:

$$K_{pq} = \frac{P_{pq}}{qH} \quad \text{Equation F.16c}$$

Combining these three equations, the ultimate passive pressure force per unit length,  $E_p$ , can be expressed in a more traditional form as:

$$E_p = \frac{1}{2}gH^2K_{pf} + 2cHK_{pc} + qHK_{pq} \quad \text{Equation F.17}$$

The value of  $E_p$  is modified in *PYCAP* for three-dimensional effects using factors developed by Ovesens (1964) from experiments on embedded anchor blocks.

The value of  $E_p$  is incorporated into a hyperbolic formulation, which is used to develop pile cap p-y values for lateral analyses. The complete process, including the generation of pile cap p-y values, is performed in the program *PYCAP*.

The  $K_{p\phi}$  value determined using the log spiral method approaches the Rankine value of  $K_p$  as  $\delta$  approaches zero. For this reason, and because numerical difficulties occasionally occur when  $\delta$  is less than 2 degrees, *PYCAP* automatically defaults to the Rankine value of  $K_p$  when  $\delta$  is less than 2 degrees. In this case, the ultimate passive force,  $E_p$ , is expressed as:

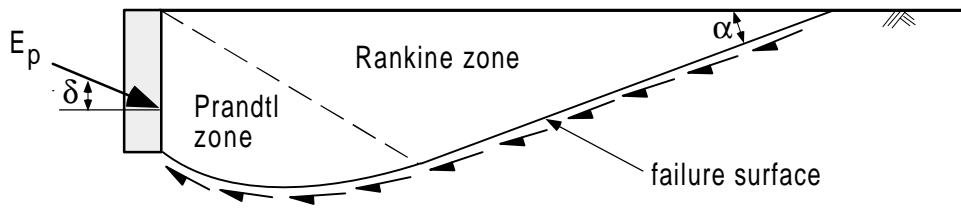
$$E_p = \frac{1}{2}gH^2K_p + 2cH\sqrt{K_p} + qHK_p \quad \text{Equation F.18}$$

where  $K_p$  is determined from Rankine theory as:

$$K_p = \tan^2\left(45 + \frac{f}{2}\right) \quad \text{Equation F.19}$$

When  $\phi = 0$ , *PYCAP* defaults to a different method for calculating  $E_p$ , which is called the  $\phi = 0$  sliding wedge method. This method is described in Appendix G.

Figure F.4 contains an example of the worksheet named *Log Spiral*, which performs the calculations described in this appendix. Values for pile cap p-y curves, created using  $P_{ult}$ , are presented in the *Summary* worksheet of *PYCAP*. An example of the *Summary* worksheet is shown in Figure F.5.

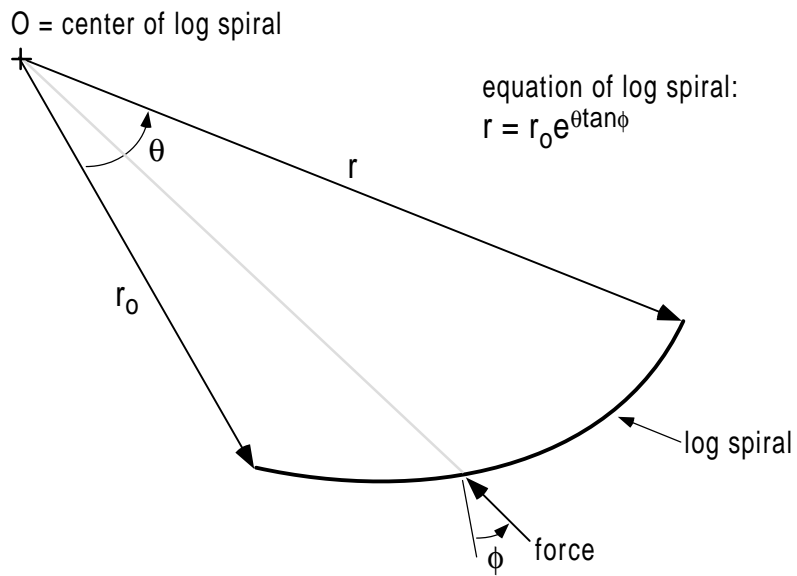


$E_p$  = passive earth pressure

$\delta$  = wall friction angle

$\alpha = 45 - \phi/2$

(a) Theoretical shape of passive failure zone.



(b) Log spiral.

Figure F.1. Log spiral approximation.

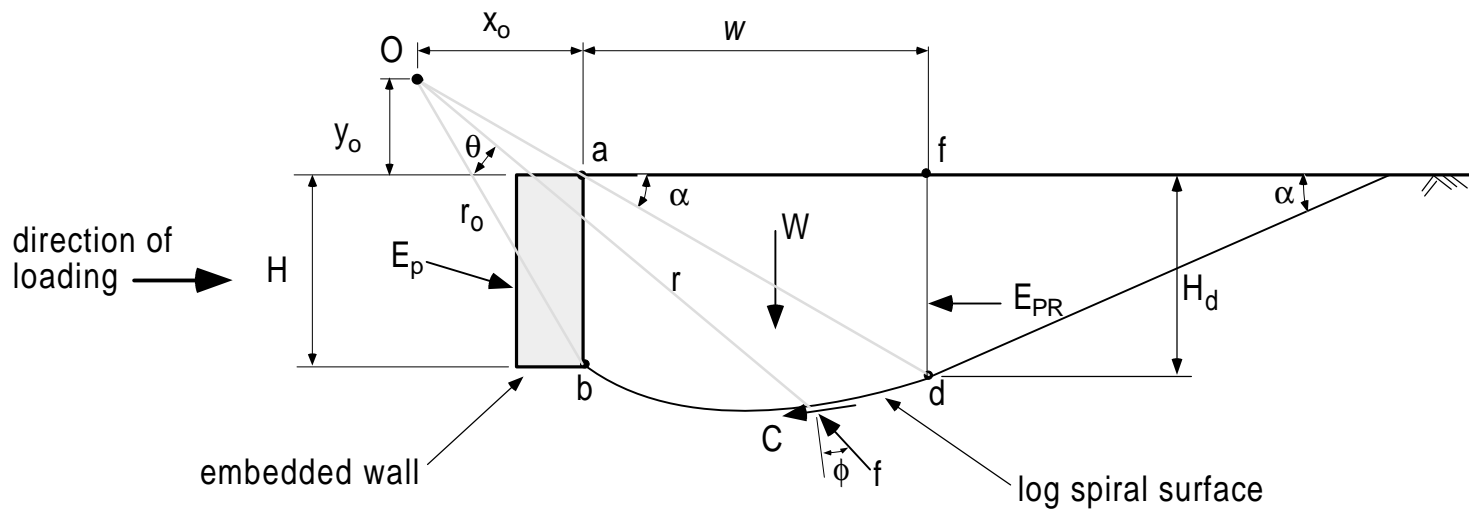
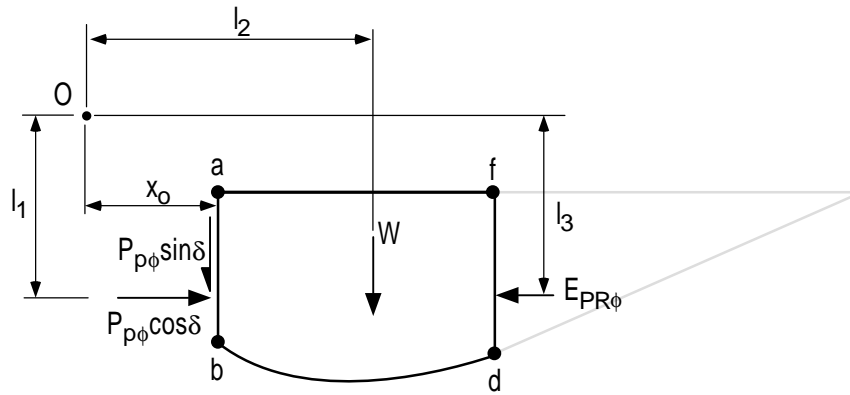
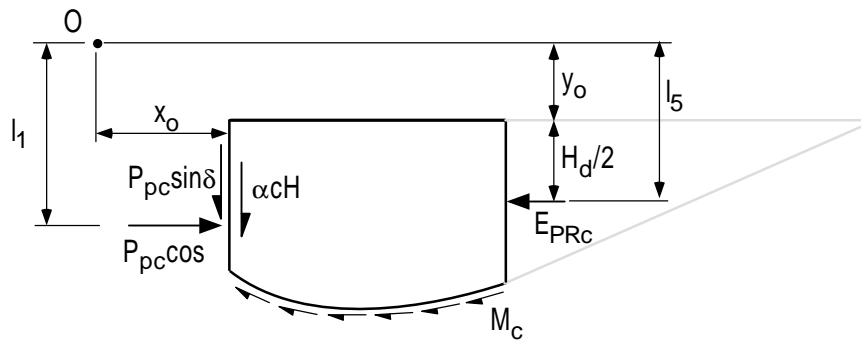


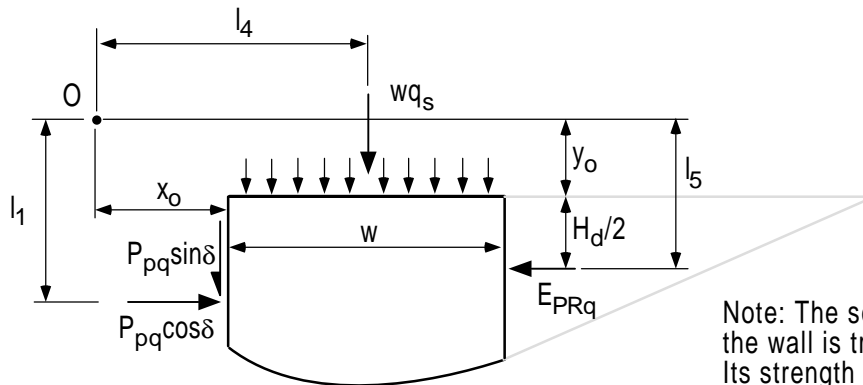
Figure F.2. Dimensions for log spiral method.



(a) Free body diagram for determining  $P_{p\phi}$ .



(b) Free body diagram for determining  $P_{pc}$ .



(c) Free body diagram for determining  $P_{pq}$ .

Note: The soil above the top of the wall is treated as a surcharge. Its strength is ignored.

Figure F.3. Free body diagrams of the log spiral failure zone.

## Log Spiral Passive Earth Pressure Calculation Worksheet

Created by R.L. Mokwa and J.M. Duncan - August 1999

Project: Bulkhead in natural soil  
 Date: 9/1/99  
 Calculated by: RLM

Enter data in column C of input table and press  
 Ctrl+a to calculate  $K_p$  and earth pressures.

**Input values - Use "summary" worksheet for data entry.**

Cap height, H (ft) =	3.50
Friction angle, $\phi$ (degrees) =	37.0
Cohesion, c (psf) =	970
Wall friction angle, $\delta$ (degrees) =	4
Unit weight, $\gamma$ (pcf) =	122
Surcharge, $q_s$ (psf) =	0.0
Adhesion factor, $\alpha$ =	0.00
Cap width, b (ft) =	6.30

**Rankine Earth Pressure Theory ( $\delta = 0$ )**

**Results**

Coefficient of active earth pressure, $K_a$ =	0.25
Coefficient of passive earth pressure, $K_p$ =	4.02
Passive force due to $\gamma$ (lb/ft) =	2,820
Passive force due to $q_s$ (lb/ft) =	0
Passive force due to c (lb/ft) =	13,619
Total passive pressure force, $E_p$ (lb/ft) =	16,439

**Log Spiral Earth Pressure Theory**

**Results**

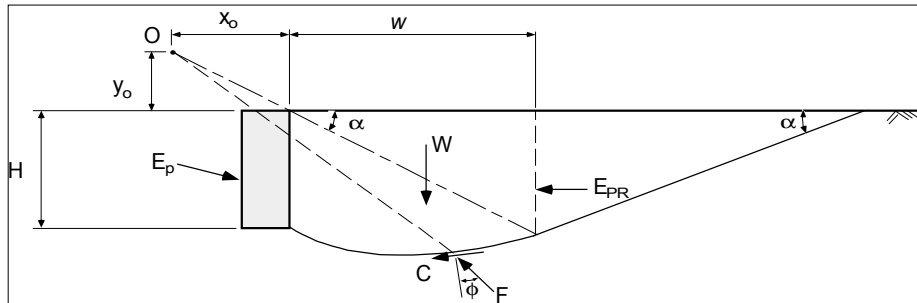
Zone width, w (ft) =	4.06
$K_{p\phi}$ =	4.65
Passive force due to $\phi$ (lb/ft) =	3,471
Passive force due to $q_s$ (lb/ft) =	-
Passive force due to c (lb/ft) =	14,343
Total passive pressure force, $E_p$ (lb/ft) =	17,814
friction, $\phi$ component $K_{p\phi}$ =	4.65
surcharge, $q_s$ component $K_{p q}$ =	0.00
cohesion, c component $K_{p c}$ =	2.11

**Coulomb Earth Pressure Theory**

**Results**

Coefficient of passive earth pressure, $K_p$ =	4.56
Passive force due to $\gamma$ (lb/ft) =	3,224
Passive force due to $q_s$ (lb/ft) =	0
Passive force due to c (lb/ft) =	14,504
Total passive pressure force, $E_p$ (lb/ft) =	17,727

**Log spiral geometric configuration used in spreadsheet calculations**



continued on next page

Figure F.4 (1 of 3). Example of *Log Spiral* worksheet.

**Block capacity using Ovesen's (1964) theory for cohesionless soil (Log Spiral).**

cap width (ft) =	6.3	$K_a = 0.25$
cap height (ft) =	3.5	$K_{p\phi} = 4.65$
overburden (ft) =	0.0	$E = 0.00$
spacing factor =	1.0	
$\gamma_{avg}$ (pcf) =	122.0	
$\phi_{avg}$ (deg) =	37.0	
B =	1.0	
Ovesen's shape factor, R =	<b>1.43</b>	
$R_{max}$ =	2	

**Capacity calculations using Log Spiral theory.**

Ult. force due to $\phi$ , $F_\phi$ , (lb) =	21867
Ult. force due to c, $F_c$ , (lb) =	90360
Ult. force due to $q_s$ , $F_q$ , (lb) =	0

**Capacity calculations applying Ovesen's (1964) 3-D shape factor to  $\phi$  and c terms.**

- Apply Ovesen's 3-D shape factor to the  $\phi$ , c, and  $q_s$  forces.
- Limit the maximum value of R to 2.0.

$$P_{ult} = R(F_\phi + F_c + F_q)$$

$P_{ult}$ (lb) =	160416
$P_{ult}$ (kips) =	<b>160</b>

**Capacity calculations for  $\phi = 0$  conditions.**

Use  $\phi = 0$  sliding wedge formulation, after Reese (1997).

$$P_{ult} = 0.5(4 + 2\alpha + \gamma H/c + 0.25H/b)cbH$$

$P_{ult}$ (lb) =	48970
$P_{ult}$ (kips) =	<b>48.97</b>

Figure F.4 (2 of 3). Example of *Log Spiral* worksheet.

**Log spiral calculations - programmed in macro.**

Intermediate value of $E_p$ =	17,814
$\alpha$ =	26.5
$H_d$ =	2.02
$x_o$ =	10.32
$y_o$ =	5.15
$r_o$ =	13.46
theta =	0.235
$r_1$ =	16.0684
$r_2$ =	16.0680
Difference between $r_1$ and $r_2$ =	0.00
$l_1$ =	7.48
a =	1.85
$l_2$ =	12.17
$l_3$ =	6.49
$l_4$ =	12.35
$l_5$ =	6.16
$\tan \phi$ =	0.754
Weight of soil, W (lb per ft) =	1,413
$\tan (45+\phi/2)$ =	2.01
Rankine $E_{PR\phi}$ (lb per ft) =	1,005
Rankine $E_{PRq}$ (lb per ft) =	-
Rankine $E_{PRc}$ (lb per ft) =	7,876
Moment due to cohesion $M_c$ (ft lb per ft) =	49,530
$\cos \delta$ =	0.998
$\sin \delta$ =	0.061
(soil weight, $\phi$ component) $P_{P\phi}$ =	3,471
(surcharge component) $P_{Pq}$ =	-
(cohesion component) $P_{Pc}$ =	14,343
$\tan (45-\phi/2)$ =	0.50

Figure F.4 (3 of 3). Example of *Log Spiral* worksheet.

## Ultimate Capacity Calculation Sheet

Created by R.L. Mokwa and J.M. Duncan - August 1999

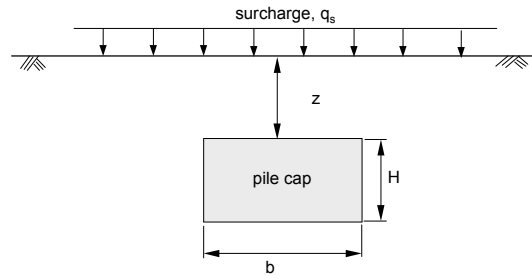
Date: 9/1/99  
 Description: Bulkhead in natural soil  
 Engineer: RLM

### Input Values (red)

cap width,	b (ft) =	6.30
cap height,	H (ft) =	3.50
embedment depth,	z (ft) =	0.00
surcharge,	$q_s$ (psf) =	0.0
cohesion,	c (psf) =	970.0
soil friction angle,	$\phi$ (deg.) =	37.0
wall friction,	$\delta$ (deg.) =	3.5
initial soil modulus,	$E_i$ (kip/ft <sup>2</sup> ) =	890
poisson's ratio,	$\nu$ =	0.33
soil unit weight,	$\gamma_m$ (pcf) =	122.0
adhesion factor,	$\alpha$ =	0.00
$\Delta_{max}/H$ , (0.04 suggested, see notes) =		0.04
<b>Calculated Values (blue)</b>		
$K_s$ (Rankine) =		0.25
$K_p$ (Rankine) =		4.02
$K_p$ (Coulomb) =		4.56
$K_{p\phi}$ (Log Spiral, soil weight) =		4.65
$K_{pq}$ (Log Spiral, surcharge) =		0.00
$K_{pc}$ (Log Spiral, cohesion) =		2.11
$E_p$ (kip/ft) =		17.81
Ovesen's 3-D factor, R =		1.43
$k_{max}$ , elastic stiffness (kip/in) =		890.5
<b><math>P_{ult}</math> (kips) =</b>		<b>160.4</b>

### Notes:

$E_p$  = passive earth pressure per foot of wall  
 $E_p = (P_{p\phi} + P_{pq} + P_{pc}) = 0.5\gamma H^2 K_{p\phi} + qHK_{pq} + 2cHK_{pc}$   
 $K_{p\phi}, K_{pq}, K_{pc}$  = Log spiral earth pressure coefficients  
 for  $\delta = 0$ ,  $E_p = 0.5\gamma H^2 K_p + qHK_p + 2cH(K)^{0.5}$   
 $P_{ult} = E_p R b$  (passive force on wall)  
 for  $\phi = 0$ ,  $P_{ult} = 0.5cbH(4 + \gamma H/c + 0.25H/b + 2\alpha)$   
 $\Delta_{max}/H$  = movement required to fully mobilize passive pressures  
 Suggested value:  $\Delta_{max}/H = 0.04$  (Clough and Duncan, 1991)



### LPILE

#### p-y values for pile cap

Depth (in) ==>	y (in)	p (lb/in)	
	0	10	<=== No. of data points
	0.00	0.0	definig p-y curves
	0.01	202.0	
	0.03	553.8	
	0.05	849.6	
	0.10	1417.7	
	0.20	2129.6	
	0.50	3048.1	
	1.00	3559.9	
	2.00	3819.4	
	10.00	3819.4	
Depth (in) ==>	42	10	<=== No. of data points
	0.00	0.0	definig p-y curves
	0.01	202.0	
	0.03	553.8	
	0.05	849.6	
	0.10	1417.7	
	0.20	2129.6	
	0.50	3048.1	
	1.00	3559.9	
	2.00	3819.4	
	10.00	3819.4	

Figure F.5. PYCAP Summary worksheet for bulkhead in natural soil.

## APPENDIX G –PASSIVE WEDGE MODEL FOR $\mathbf{f} = 0$

This appendix describes the formulation for estimating the ultimate passive resistance,  $P_{ult}$ , that is developed in  $\phi = 0$ , cohesive soils. The method follows closely the approach developed by Reese (1997) for modeling the failure zone in front of a laterally loaded pile. This approach assumes that the ground surface rises and translates in the direction of load. The failure wedge is assumed to be a plane surface, as shown in Figure G.1.

The equations developed in this appendix are used in the spreadsheet *PYCAP* for calculating the ultimate passive force developed in front of a pile cap for  $\phi = 0$  soils. For  $\phi > 0$  or  $c-\phi$  soils, the log spiral method described in Appendix F was used.

$P_{ult}$  is determined from equilibrium of the forces shown in Figure G.1. These forces are defined below.

Body force, or weight of soil in the failure wedge =  $W$ .

$$W = \frac{1}{2} \mathbf{g}bH^2 \tan \mathbf{q} \quad \text{Equation G.1}$$

Shear force between cap and wedge =  $F_f$ .

$$F_f = \mathbf{a}cbH \quad \text{Equation G.2}$$

where  $\alpha c$  is the adhesion between the cohesive soil and wall.

Shear force on bottom of sliding wedge =  $F_s$ .

$$F_s = \frac{cbH}{\cos \mathbf{q}} \quad \text{Equation G.3}$$

Shear force on side of sliding wedge =  $F_t$ .

$$F_t = \frac{1}{2} cH^2 \tan \mathbf{q} \quad \text{Equation G.4}$$

Normal force acting on bottom of sliding wedge,  $F_n$ , is determined by summing forces in the vertical direction:

$$F_n = \frac{1}{2}gbH^2 \frac{1}{\cos q} + acbH \frac{1}{\sin q} + cH^2 + \frac{cbH}{\sin q} \quad \text{Equation G.5}$$

Ultimate passive force,  $P_{ult}$ , is determined by summing forces in the horizontal direction:

$$P_{ult} = cbH \frac{\sin q}{\cos q} + cH^2 \frac{\sin^2 q}{\cos q} + \frac{1}{2}gbH^2 + acbH \frac{\cos q}{\sin q} + cH^2 \cos q + cbH \frac{\cos q}{\sin q} \quad \text{Equation G.6}$$

Angle of failure wedge =  $\alpha$ .

$$a \approx 45 + \frac{f}{2} \quad \text{Equation G.7}$$

For the case of  $\phi = 0$ ,  $\alpha \approx 45$  degrees. Making this substitution into Equation G.7 results in:

$$P_{ult} = \frac{cbH}{2} \left( 4 + 2a + \frac{gh}{c} + \frac{2.8H}{b} \right) \quad \text{Equation G.8}$$

Reese (1997) modified Equation G.8 based on results of fullscale tests performed by Matlock (1970). Reese's semi-empirical equation for the soil resistance per unit length, assuming a linear increase with depth, is given as:

$$p_{ult} = \frac{2P_{ult}}{H} = cb \left( 3 + \frac{gx}{c} + \frac{Jx}{b} \right) \quad \text{Equation G.9}$$

where  $x$  is the depth below ground surface. Matlock determined the value of  $J$  to be 0.5 for soft clay and about 0.25 for medium stiff clay. Reese assumed that because of cyclic loading,  $\alpha = 0$ . Integrating Equation G.9 with respect to  $x$ , between the limits of  $x = 0$  and  $x = H$ , results in the following expression for  $P_{ult}$ :

$$P_{ult} = \frac{cbH}{2} \left( 6 + \frac{gH}{c} + \frac{JH}{b} \right) \quad \text{Equation G.10}$$

Reese's (1997) semi-empirical equation for  $P_{ult}$ , Equation G.10, is similar in form to Equation G.8, except that Reese's equation (G.10) does not contain a term for adhesion,  $\alpha c$ , and some of the constant values have been adjusted, presumably to match the results of Matlock's (1970) pile load tests. The effects of soil adhesion are implicitly included in Equation G.10 for the piles that were used in Matlock's (1970) study. However, this expression may not accurately reflect the influence that adhesion has on pile caps, which are typically much wider than Matlock's test piles (which were 13 inches in diameter). For this reason, a modified version of the theoretical expression was used by Reese and Matlock with the term  $2.8H/b$  replaced by  $JH/b$ . Because soft clays are seldom used as backfill around pile caps,  $J$  was assumed to equal 0.25 (Matlock's recommendation for medium stiff clays.)

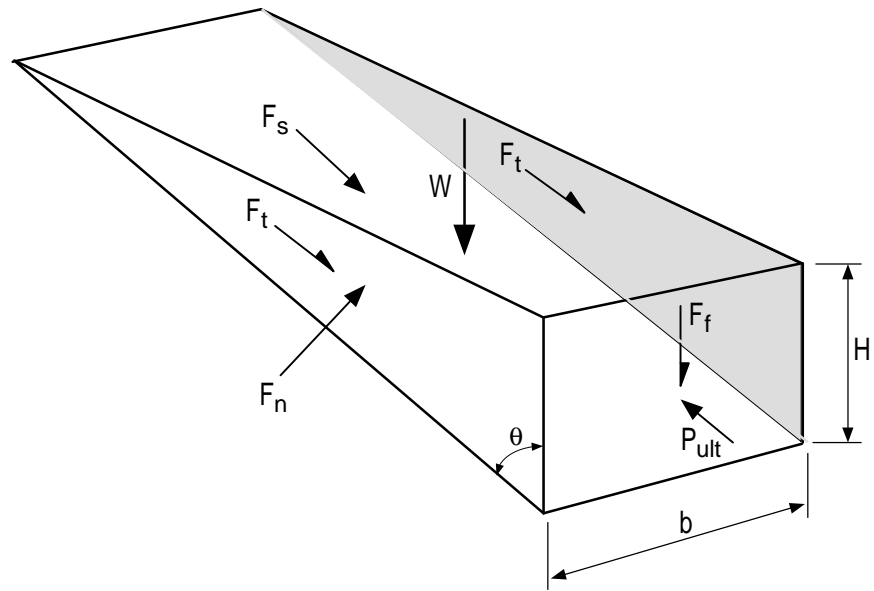
Changing the coefficient of the last term in equation G.8 from 2.8 to 0.25, based on Matlock's recommendation, results in the following expression for calculating  $P_{ult}$  for undrained,  $\phi = 0$ , conditions:

$$P_{ult} = \frac{cbH}{2} \left( 4 + 2a + \frac{gH}{c} + \frac{0.25H}{b} \right) \quad \text{Equation G.11}$$

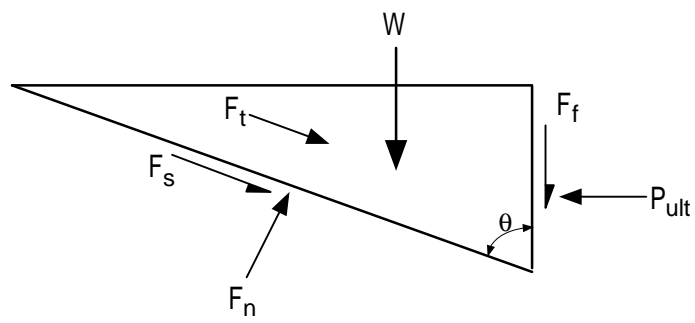
This expression provides results that are consistent with the log spiral/Ovesen approach (described in appendix F) for small values of  $\phi$  and  $\delta$ . For example, for a 5-foot-wide, 3-foot-deep cap with  $c = 1000$  psf,  $\gamma = 120$  pcf,  $\alpha = 0$ , and  $\phi = 0$ ,  $P_{ult}$  determined from Equation G.11 is 33.8 kips. In comparison, using the modified log spiral approach with  $\phi = \delta = 2^\circ$  resulted in  $P_{ult}$  equal to 34.0 kips. Calculations for  $\phi = 0$  conditions are performed in the worksheet named *Log Spiral*, which is part of the *PYCAP* workbook.

In summary, Equation G.11 was used in this study to calculate the ultimate resistance of pile caps for  $\phi = 0$  soil conditions. The program *PYCAP* automatically defaults to this expression whenever  $\phi = 0$ . The calculated  $P_{ult}$  value is incorporated into a hyperbolic

formulation, which is used for developing p-y curve values for pile cap analyses. The entire process, including the generation of pile cap p-y values, is automated in the program *PYCAP*.



Orthogonal view of failure wedge



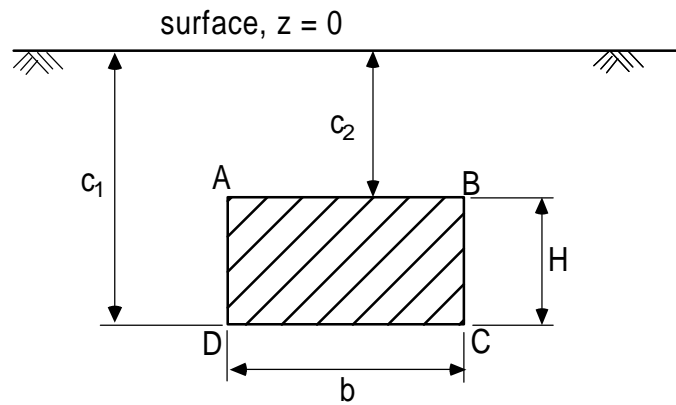
Side view of failure wedge

Figure G.1.  $\phi = 0$  passive wedge model,

## APPENDIX H – EQUATIONS FOR COMPUTING THE INITIAL ELASTIC STIFFNESS, $k_{\max}$

### H.1 Introduction

This Appendix presents the equations that were used to compute the initial elastic stiffness for the pile caps,  $k_{\max}$ . The method is based on elasticity equations developed by Douglas and Davis (1964) for calculating the horizontal displacement,  $y$ , at the upper and lower corners of a rectangular area in a semi-infinite, isotropic, homogeneous, elastic half-space. The dimensions that are used in the equations are shown in the sketch below.



### H.2 Equations for Calculating Deflection

For a uniform horizontal pressure,  $p$ , the deflection,  $y_1$  at upper corners A and B is given by equation H.1. The deflection,  $y_2$ , at lower corners C and D is given by Equation H.2.

$$y_1 = \frac{pb(1-n)}{16pE_i(1-n)} \{(3-4n)F_1 + F_4 + 4(1-2n)(1-n)F_5\} \quad \text{Equation H.1}$$

$$y_2 = \frac{pb(1-n)}{16pE_i(1-n)} \{(3-4n)F_1 + F_2 + 4(1-2n)(1-n)F_3\} \quad \text{Equation H.2}$$

where:

$p$  = uniform horizontal pressure applied to the rectangular area ABCD,

$\nu$  = Poisson's ratio,

$E_i$  = initial soil tangent modulus,

$b$  = cap width, and

$F_1$  through  $F_5$  = influence factors defined in Section H.3.

### H.3 Equations for Calculating Influence Factors $F_1$ Through $F_5$

$$F_1 = -(K_1 - K_2) \ln \left( \frac{K_1 - K_2}{2 + \sqrt{4 + (K_1 - K_2)^2}} \right) - 2 \ln \left( \frac{2}{(K_1 - K_2) + \sqrt{4 + (K_1 - K_2)^2}} \right) \quad \text{Equation H.3}$$

$$F_2 = 2 \ln \left( \frac{2(K_1 + \sqrt{1 + K_1^2})}{(K_1 + K_2) + \sqrt{4 + (K_1 + K_2)^2}} \right) + (K_1 + K_2) \ln \left( \frac{2 + \sqrt{4 + (K_1 + K_2)^2}}{(K_1 + K_2)} \right) - K_1^2 \left( \frac{\sqrt{4 + (K_1 + K_2)^2}}{(K_1 - K_2)} - \frac{\sqrt{1 + K_1^2}}{K_1} \right) \quad \text{Equation H.4}$$

$$F_3 = -2K_1 \ln \left( \frac{K_1}{1 + \sqrt{1 + K_1^2}} \right) + (K_1 + K_2) \ln \left( \frac{(K_1 + K_2)}{2 + \sqrt{4 + (K_1 + K_2)^2}} \right) - \ln \left( \frac{(K_1 + K_2) + \sqrt{4 + (K_1 + K_2)^2}}{2(K_1 + \sqrt{1 + K_1^2})} \right) + \frac{(K_1 + K_2)}{4} \left[ \sqrt{4 + (K_1 + K_2)^2} - (K_1 + K_2) \right] - K_1 \left( \sqrt{1 + K_1^2} - K_1 \right) \quad \text{Equation H.5}$$

$$F_4 = -2 \ln \left( \frac{2(K_2 + \sqrt{1 + K_2^2})}{(K_1 + K_2) + \sqrt{4 + (K_1 + K_2)^2}} \right) + (K_1 - K_2) \ln \left( \frac{2 + \sqrt{4 + (K_1 + K_2)^2}}{(K_1 + K_2)} \right)$$

$$+ K_2^2 \left( \frac{\sqrt{4 + (K_1 + K_2)^2}}{(K_1 + K_2)} - \frac{\sqrt{1 + K_2^2}}{K_2} \right) \quad \text{Equation H.6}$$

$$F_5 = 2K_2 \ln \left( \frac{K_2}{1 + \sqrt{1 + K_2^2}} \right) - (K_1 + K_2) \ln \left( \frac{K_1 + K_2}{2 + \sqrt{4 + (K_1 + K_2)^2}} \right) \\ + \ln \left( \frac{(K_1 + K_2) + \sqrt{4 + (K_1 + K_2)^2}}{2(K_2 + \sqrt{1 + K_2^2})} \right) - \left( \frac{K_1 + K_2}{4} \right) \\ \times \left( \sqrt{4 + (K_1 + K_2)^2} - (K_1 + K_2) \right) - K_2 \left( K_2 - \sqrt{1 + K_2^2} \right) \quad \text{Equation H.7}$$

where:

$$K_1 = \frac{2c_1}{b},$$

$$K_2 = \frac{2c_2}{b},$$

$c_1$  = depth to bottom of rectangular area, and

$c_2$  = depth to top of rectangular area.

The displacement at other points within plane ABCD can be determined using interpolation, assuming deflections vary linearly over the loaded area..

#### H.4 Equations for $k_{\max}$

$k_{\max}$  is the slope of the load-deflection curve. The load versus deflection relationship computed using Douglas and Davis's (1964) elasticity equations is linear. Thus,  $k_{\max}$  is the applied load divided by the corresponding deflection of the cap. The applied load, P, or horizontal force on the cap is given by Equation H.8 as:

$$P = p(b)(h) \quad \text{Equation H.8}$$

where  $p$  is the applied horizontal pressure,  $b$  is the cap width, and  $h$  is the cap depth.

The average deflection at the top corner and the bottom corner of the cap,  $y_c$ , is:

$$y_c = \frac{y_1 + y_2}{2} \quad \text{Equation H.9}$$

The initial elastic stiffness,  $k_{\max}$ , is the slope of the load-deflection curve, given by Equation H.10, as:

$$k_{\max} = \frac{P}{y_c} \quad \text{Equation H.10}$$

The units of  $k_{\max}$  are force per length, [F/L].